SUPPORTING INFORMATION

Ratiometric imaging using a single dye enables simultaneous visualization of Rac1 and Cdc42 activation

Christopher J. MacNevin,† Alexei Toutchkine,† Daniel J. Marston, Chia-Wen Hsu, Denis Tsygankov, Li Li, Bei Lui, Timothy Qi, Dan-Vinh Nguyen, and Klaus M. Hahn*

Department of Pharmacology, The University of North Carolina at Chapel Hill, Chapel Hill, North Carolina 27599, United States

Supporting Figures

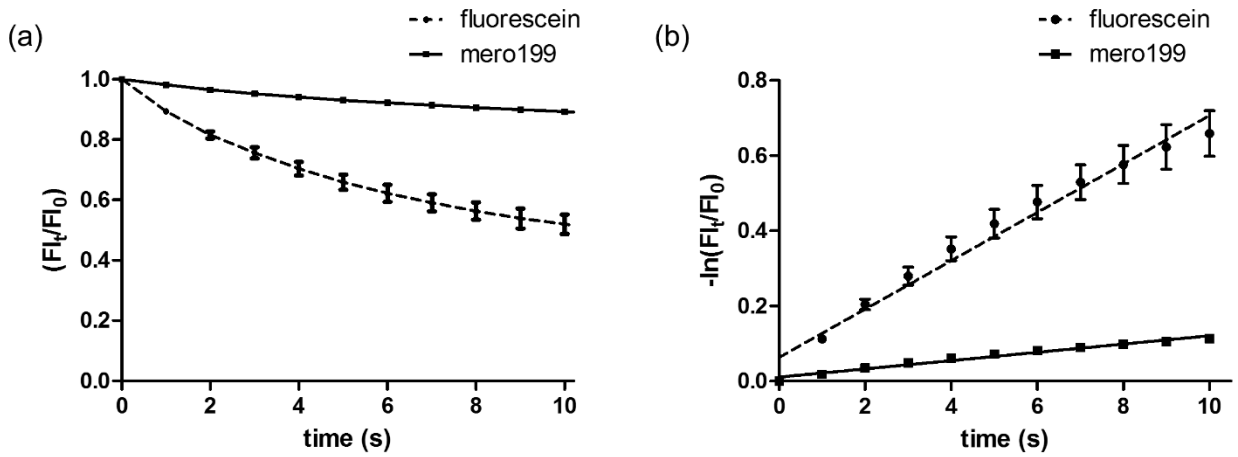

Figure S1. Fluorescence decay (a) and decay rate (b) due to photobleaching. Samples were prepared at 1.0 µM in 1% agarose/TAE as a thin layer between two glass coverslips. Samples were imaged on an Olympus IX71 inverted microscope equipped with a 100×, 1.45 NA oil objective (Olympus PLAN APO). Fluorescence signals were acquired using an electron-multiplying charge-coupled device (EMCCD) camera (Andor iXon DV-897 Ultra). A super-continuum laser source (Fianium) equipped with an AOTF was adopted for the excitation of different dyes. Laser intensities were kept at ~1.4 mW at the rear pupil of the objective for both 488 nm and 565 nm. Laser irradiation was maintained continuously throughout the experiment. The exposure time was maintained at 200 ms and the sampling rate was 1 Hz for **mero199** and 2 Hz for fluorescein. The photobleaching rate was calculated as the slope of -ln (Fl_t/Fl_0) vs. time, to give 0.064 ($\underline{\pm}$ 0.004) for fluorescein and 0.011 (± 0.001) for **mero199** (n = 3 runs).

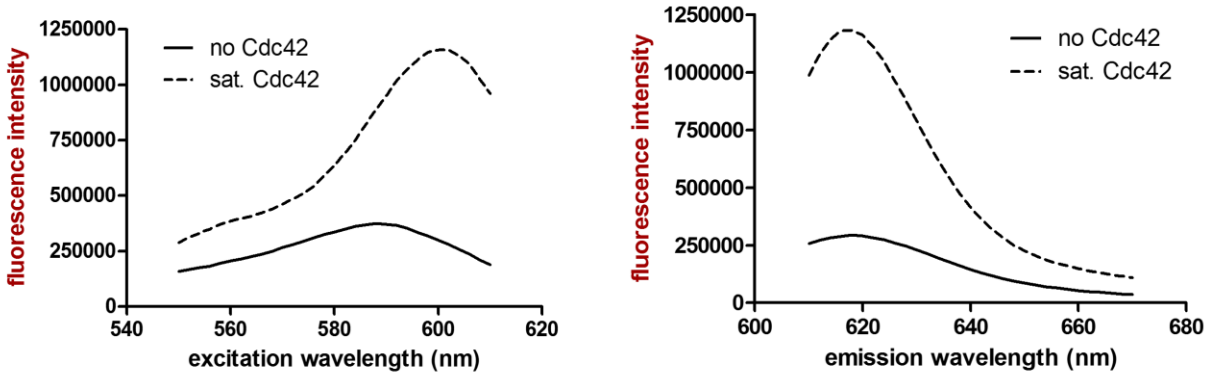

Figure S2. Excitation and emission spectra of **CRIB199** with no Cdc42 and with saturating Cdc42 (1.60 µM).

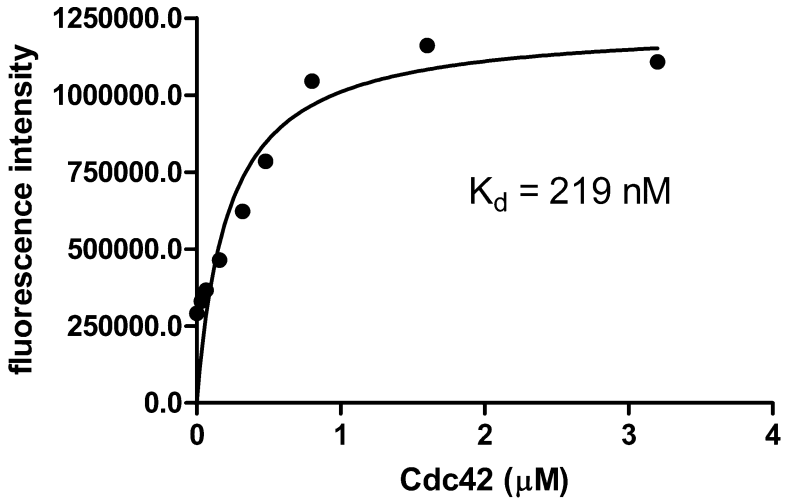

Figure S3. In vitro binding of the **CRIB199** sensor to Cdc42. (a) Cdc42 binding affinity of the **mero199**-CBD conjugate.

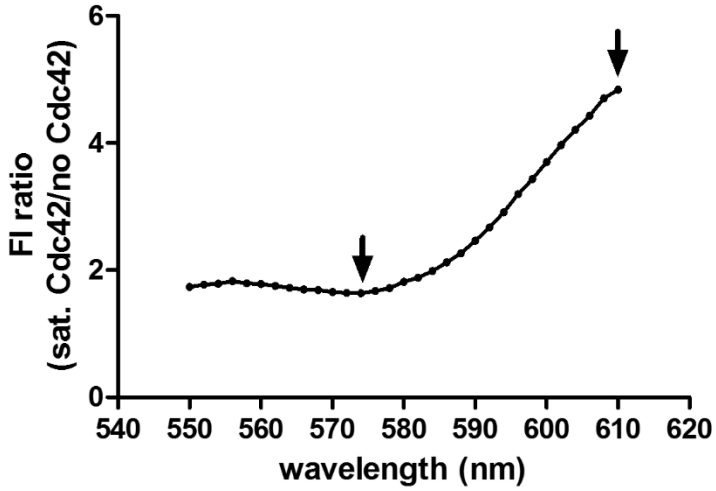

Figure S4. Ratio of excitation with and without saturating Cdc42 and no Cdc42. Arrows along the curve indicate the wavelengths used for imaging studies (577/10 and 605/15 nm filters).

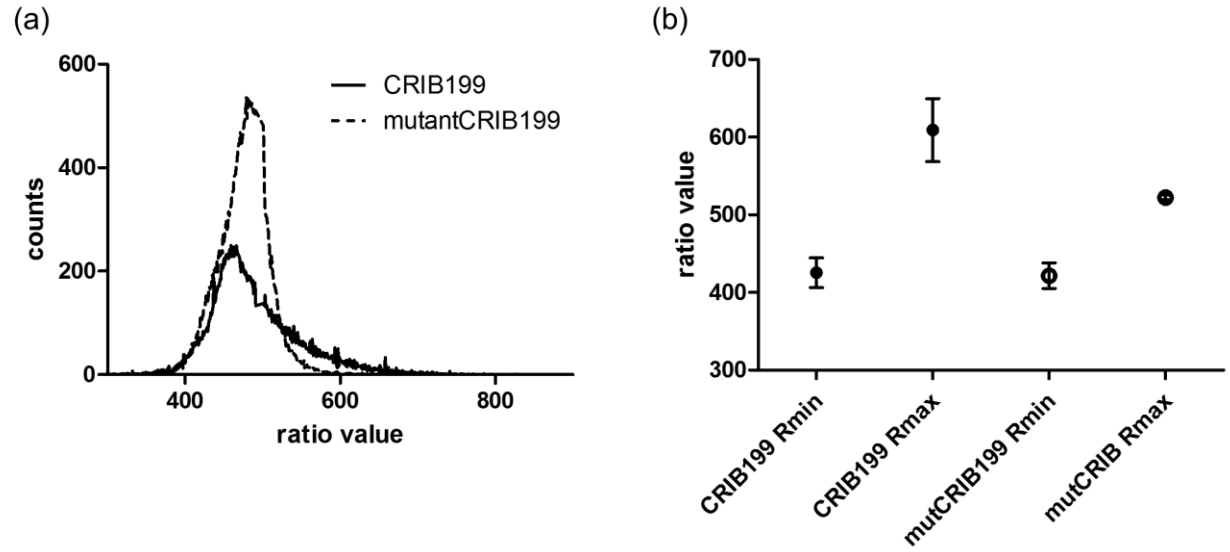

Figure S5. Quantification of dynamic range using ratio values within images. (a) Histograms of ratio values within CRIB199 and mutantCRIB199 images (plots are average of 3 cells per biosensor). (b) Ratio value minimum (Rmin) was taken as the ratio where only 5% of pixels had lower values, and ratio value maximum (Rmax) was the ratio where only 5% of the pixels had higher values. This approach eliminates artifactual high or low pixels. The Rmin and Rmax values are sensitive to the percentage values chosen, the nature of the broad band pass filters used for imaging, and the extent to which the cell contains pixels where biosensor is fully saturated with Cdc42. Therefore the dynamic range for CRIB199 is equal to or greater than that shown here, consistent with the data in Figure S2. CRIB199: Rmin = 425.0 ± 11.36; Rmax = 609.0 ± 23.43 (n = 3 cells). mutCRIB199: Rmin = 422.3 ± 9.8; Rmax values = 522.3 ± 1.8 (n = 3 cells).

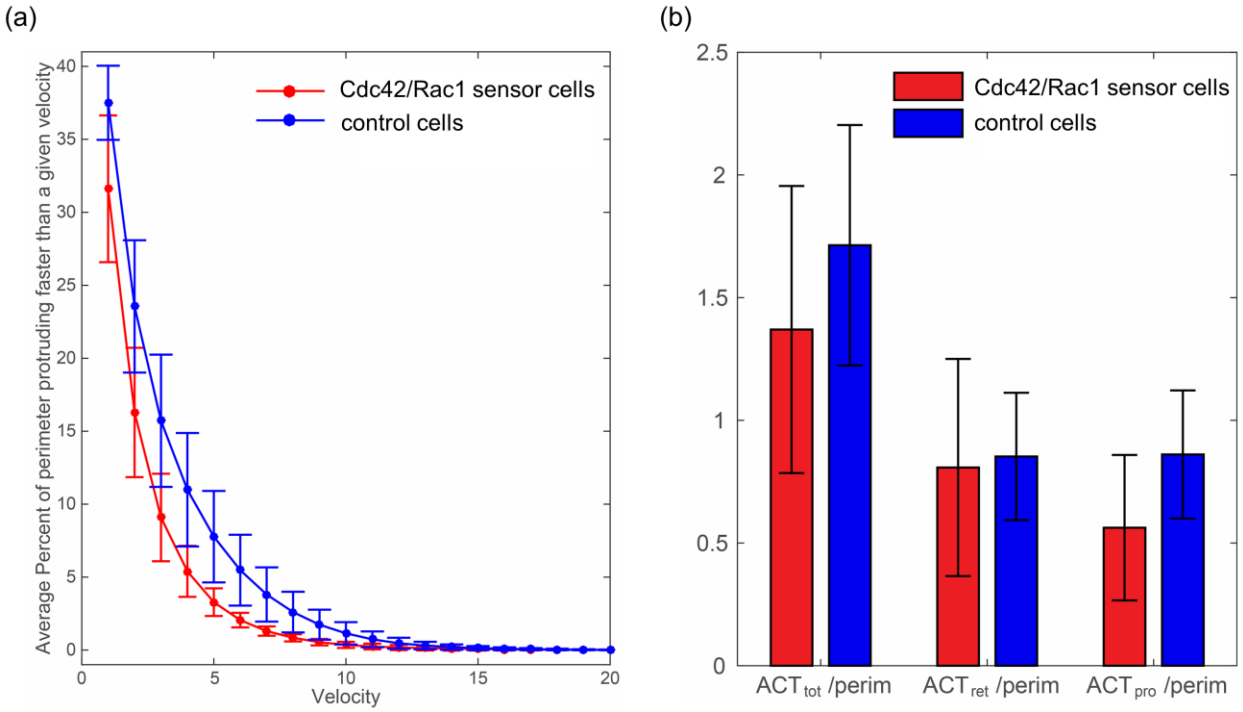

Figure S6. Measures of protrusive activity in cells containing either no biosensor (blue) or cells containing both the Cdc42 and Rac1 biosensors (red). (a) Percent of perimeter protruding faster than a given velocity (biosensor: n = 6 cells, control: n = 8 cells). (b) Measure of protrusive activity (total, retraction only, and protrusion only) averaged over all time points of all cell tracks (biosensor: n = 6 cells, control: n = 8 cells). Error bars indicate standard deviations of the mean.

Molecular biology, imaging, and image analysis methods

Protein expression. The Cdc42-binding domain (CBD), derived from Wiskott-Aldrich syndrome protein (WASP, residues 201-320), was mutated to include a single cysteine (F271C) for dye attachment and fused at its C-terminus with maltose-binding protein (MBP) to enhance solubility, using a GSGSGS linker. The CBD mutant that cannot bind to the active form of Cdc42 carries the additional mutations H246D and H249D. CBD-MBP and CBD-MBP inactive mutant fragments were each subcloned into a pET23b plasmid to generate a C-terminal 6xHis fusion protein. The constitutively active Cdc42 mutant, Cdc42 Q61L, was subcloned into the pQE-80L plasmid to generate an N-terminal 6xHis fusion protein. The resulting constructs were transformed into the BL21(DE3) strain from *E. Coli* (Stratagene) and the bacteria were cultured at 37 °C, 245 rpm in Leuria-Bertani medium in the presence of 100 µg/mL carbenicillin until OD600 reached 0.8. Protein expression was conducted at 23 °C for 5 hours after addition of β-D-1-thiogalactopyranoside (IPTG) to final concentration of 40 µM. The bacterial pellet was collected by centrifugation at 4000 rpm for 20 min, 4 °C, and stored at -80 °C prior to purification.

Protein purification. For lysis, the bacterial pellets were resuspended in 30 mL of lysis buffer (50 mM NaH_2PO_4, pH 7.0, 300 mM NaCl) and disrupted by sonication. The supernatant was collected by centrifugation at 6000 rpm for 15 min, 4 °C, followed by incubation with Talon Metal Affinity Resin (Clontech) on a nutator mixer for 1 hour at 4 °C. The protein-bound resin was collected after centrifugation at 1600 rpm for 2 min, 4 °C, washed with the lysis buffer (3 X) to remove non-specifically bound proteins, and loaded onto a polypropylene column (BioRad). The immobilized proteins were washed with 20 mL of the washing buffer (50 mM NaH_2PO_4, pH 7.5) and eluted with 1~2 mL elution buffer (300 mM imidazole, pH 7.0). To fully reduce the F271C residue of CBD-MBP, 1µl of β-mercaptoethanol (BioRad) was added to the eluate and the resulting protein solution was concentrated to 200 µl by centrifuge. The imidazole and β-mercaptoethanol were removed by buffer exchange on a dextran desalting column (Thermo Scientific Pierce, 5K MWCO) using the protein labeling buffer (50 mM NaH_2PO_4, pH 7.5). The protein aliquots were stored at -80 °C.

Protein labeling and in vitro binding assay. Freshly prepared CBD-MBP (100 µL of a 132.5 µM stock solution in 50 mM sodium phosphate buffer, pH 7.5) or CBD-MBP non-binding mutant (100 µL of 155.4 µM stock) was mixed with approximately 5 molar equivalents of **mero199** (3 uL of 20 - 25 mM DMSO solution) and gently mixed at room temperature for 2 h. The reaction was quenched by adding 1 µL of β-mercaptoethanol. Excess dye was removed by passing the reaction mixture through a 1 x 20 cm Sephadex G-15 (Sigma-Aldrich) column pre-equilibrated with 50 mM sodium phosphate buffer, pH 7.5. The column was wrapped in aluminum foil to minimize exposure to light. Labeling efficiency and concentrations of CBD-MBP and CBD-MBP non-binding mutant dye conjugates were determined using absorption measurements at protein maximum absorption in labeling buffer (CBD-MBP abs max = 280 nm, extinction coefficient (ε) = 74830 M^{-1} cm^{-1}) and dye maximum absorption wavelength in DMSO (**mero199** abs max = 596, ε = 190000). Samples were prepared by mixing various concentrations of Cdc42 Q61L (constitutively active mutant) in a 150 mM NaCl, 50 mM sodium phosphate buffer, pH 7.5 to reach a final volume of 400 uL with CBD-MBP final concentration at 400 nM. Fluorescence intensity measurements (excitation at 600 nm) were taken after incubation of samples for 10 min at room temperature.

Cell culture and microinjection. NIH 3T3 mouse embryonic fibroblasts (MEF) were maintained in 10% CO_2 at 37°C in Dulbecco's modified Eagle's medium (DMEM, Cellgro) with

10% fetal bovine serum (HyClone, Thermo Scientific) and 2 mM GlutaMax (Gibco, Life Technologies). The cells were plated on coverslips that had been coated with 20 µL/mL fibronectin (Sigma-Aldrich) in DPBS (Corning/Cellgro) overnight. Micropipettes were made fresh with a flaming/brown micropipette puller (Sutter Instrument Co., Model P-97) and thin-walled glass capillary tubes (World Precision Instruments, 1.2 O.D./ 0.9 I.D., TW120F-4). Cells were microinjected on an inverted microscope (Zeiss Axiovert S100 TV) with a 40X objective (LD Achrostigmat, 0.30 N.A., Ph1), followed by recovery at 37 °C in the cell incubator in Ham's F-12K medium without phenol red (Gibco) with 5% fetal bovine serum, 15 mM HEPES, and 2mM GlutaMax for at least 30 min prior to imaging.

Ratiometric image acquisition. Live cell imaging was carried out on an Olympus IX81 microscope with a UPLFLN 40X oil objective (NA 1.3) and mercury lamp excitation (103W HBO bulb). Excitation was through a ND1.5 (3% transmission) neutral density filter, with 200 ms exposure. For **mero199**, filters were as follows: 577/10 excitation 1 (Chroma), 605/15 excitation 2 (Semrock), and 630/45 emission (Chroma). Images were acquired with a Coolsnap ES2 camera (Photometrics) with a Sony 6.45 x 6.45 ìM/pixel chip using 2 x 2 binning. All image acquisition, processing, and analysis was carried out with Metamorph software. The lowest value of the pseudo-color scale was set based on a histogram of ratios within the entire cell, with 1.0 set at the 5% histogram level.

Rac1 biosensor and cell culture. Rac1 FLARE biosensor is a modification of the dual chain biosensor designs previously described in Machacek et al.[1] Turquoise fluorescent protein replaced CyPet to improve brightness and FRET efficiency.[2] The two biosensor chains were expressed on one open reading frame with two consecutive 2A viral peptide sequences from porcine teschovirus-1 (P2A) and Thosea asigna virus (T2A) inserted between them, leading to cleavage of the two chains during translation.[3] The biosensor constructs were inserted into a Tet-off inducible retroviral expression system and stable lines were produced in Tet-off MEFs (Mouse Embryonic Fibroblasts, Clontech). Cells were maintained in DMEM (Cellgro) with 10% FBS (Hyclone) in 10% CO_2 at 37ºC with 0.2µg/ml doxycycline to repress biosensor expression and used at passage 12-30. For imaging of **CRIB199** alone, the same cells without the Rac1 biosensor were used.

Microinjection and image acquisition. Biosensor expression was induced in MEFs 48h prior to imaging by trypsinization and culturing without doxycycline. Two hours prior to microinjection, cells were then re-plated on glass coverslips that were coated with 5 µg/mL of bovine fibronectin (Sigma-Aldrich) at 37°C overnight. Micropipettes were made fresh with a flaming/brown micropipette puller (Sutter Instrument Co., Model P-97) and thin-walled glass capillary tubes (World Precision Instruments, 1.2 O.D./ 0.9 I.D., TW120F-4). Cells were microinjected with 50 uM dye labelled CRIB on an inverted microscope (Ziess Axiovert S100 TV) with a 40X objective (LD Achrostigmat, 0.30 N.A., Ph1), followed by recovery at 37 °C for 30mins in an incubator in Hams F-12(K) (Caisson Labs) with 5% FBS and 10 mM Hepes (Gibco). Time-lapse images were acquired every 20 seconds on an Olympus IX81 inverted epifluorescence microscope fitted with temperature control (BC-100 20/20 Technology). For dual imaging, cells were imaged using an Olympus 40x UPlan FLN1.25 N/A silicon oil objective and Flash 4 sCMOS camera (Hamamatsu). For **CRIB199** alone, cells were imaged using a UPLFLN 40X oil objective (NA 1.3) and a Coolsnap ES2 camera (Photometrics). Cells were illuminated with a 100 W Hg arc lamp through a neutral density UVND 1.5 filter. For emission ratio imaging of Rac1, the following filter sets were used (Semrock): CFP: (ex)FF-434/17, (em)FF-482/35; FRET: (ex)FF-434/17, em(FF-550/49); YFP: (ex) FF-510/10,em(FF-550/49).). For **mero199**, filters were as follows: 577/10 excitation 1 (Chroma), 605/15 excitation 2

(Semrock), and 630/45 emission (Chroma), all using a tri band dichroic FF444/521/608 (Semrock).

Biosensor image processing. Rac1 activation levels were measured in living cells by monitoring the ratio of FRET to CFP emission, corrected for bleed-through from CFP and YFP as previously described.[1] Matlab software was used for bead based alignment of donor and FRET images, and for ratiometric calculation of activation signals. Images were shade-corrected, and then background-subtracted. Control cells expressing either donor or acceptor alone were used to obtain the bleed-through coefficients α and β in the following equation: $R = (FRET - \alpha(CFP) - \beta(YFP))/CFP$**,** where R is the Ratio, FRET is the total FRET intensity as measured, α is the bleed-through of the donor into the FRET signal, β is the bleed-through of acceptor into the FRET signal, and CFP and YFP are the donor and acceptor intensities as measured through direct excitation. Images were scaled based on the histogram analysis method described in Figure S5.

Image analysis. The correlation between cell edge velocity and biosensor activity at the edge was analyzed using our new user-friendly software EdgeProps. EdgeProps is a MATLAB-based graphical user interface (GUI) designed for visualization and analysis of cell edge dynamics in relationship with spatiotemporal distributions of the intracellular fluorescence signal. The GUI requires selection of two tiff files of image stacks with the florescence data and cell masks (if the data are pre-processed to set the background to zero, the same file can be use as the masked image set). Upon image loading the program extracts the cell edge at each time frame as an equilateral contour around the cell mask, which was smoothed with a Gaussian filter (sigma = 1 pixel). At the next step, "edge analysis", the program calculates: 1) activity at the edge, as an average non-background signal in a disk of user-defined radius with the center at each point of the contour at each time frame; 2) edge velocity, as a minimum-distance displacement of the contour points at time *t* with respect to the position of the cell contour at time *t*+*lag*, where *lag* is a user-defined parameter; 3) angular orientation of the edge points (0 to π) with respect to the rightward direction from the cell centroid. Each pair of the calculated quantities can be visualized side-by-side as the cell contours are colored according to the corresponding values. This way, for example, the velocity and biosensor activity can be visually compared in the same static view at each time frame without running the movie back and forth in an attempt to visually assess the correlation between these quantities. The quantitative correlation between activity, velocity, and orientation is displayed as a colormap view of the two-dimensional histogram made of the pairs of values from all contour points and all time frames. This colormap is overlaid with a correlation curve calculated by averaging the bins along one of the 2D-histogram directions.

The activity profiles for both Cdc42 and Rac1 biosensors were normalized for each cell across the whole range of velocities (both negative and positive) such that activity at 0 velocity is 0 and activity at large positive velocity (4 um/min in our case) is 1. This normalization makes activity values that are smaller than the value at 0 velocity negative. The formula used for normalization is as follows: normalized activity(V) = (activity(V) – activity(V=0)) / (activity(V=4) – activity(V=0)).

Other features of EdgeProps (although not presented in this work) include: 1) kymograph representation of the data, in which calculated quantities at the edge from each time frame are stacked to obtain colormaps with the cell perimeter and time as the axes; and 2) interior analysis, in which the activity and orientation are calculated for each pixel inside the cell in the same way as in the edge analysis, but the velocity is interpolated from the edge using a steep Hill function (with a user-defined Hill coefficient). This software is freely available from the Hahn Lab website: http://www.hahnlab.com/tools.

Experimental procedures and spectroscopic data for new compounds

General materials and methods. 2,3,3-Trimethylindolenine was purchased from TCI America. All other reagents were purchased from Sigma-Aldrich. 5-(3-Methoxy-allylidene)-1,3-dimethyl-pyrimidine-2,4,6-trione was prepared according to a previously reported procedure.[4] Reactions were run using anhydrous solvents. All operations with dyes were performed under dim light. UV-visible spectra were obtained with a Hewlett-Packard 8453 diode array spectrophotometer. HPLC separations were performed on Shimadzu Prominence system using a 250 x 21.2 mm, 15 micron Phenomenex C18 preparative column and elution at 8 mL/min with a gradient of 10% solvent B (H_2O/ACN 5:95, TFA 0.05%) 90% solvent A (H_2O/ACN 95:5, TFA 0.05%) for 2 min, increasing to 90% solvent B over 30 min and held for a total of 45 min. Emission and excitation spectra were obtained using a Spex Fluorolog 2 spectrofluorometer at room temperature. Mass spectra were obtained on a Hewlett-Packard 1100 or Agilent QTOF mass-selective detector (MS-ESI) using direct infusion. NMR spectra were obtained on Varian Mercury-300 or Inova-400 spectrometers. Chemical shifts are reported using NMR reference peaks of 7.26 (^{1}H) and 77.23 (^{13}C) ppm for $CDCl_3$, and 2.50 (^{1}H) and 39.51 (^{13}C) ppm for DMSO-d_6.

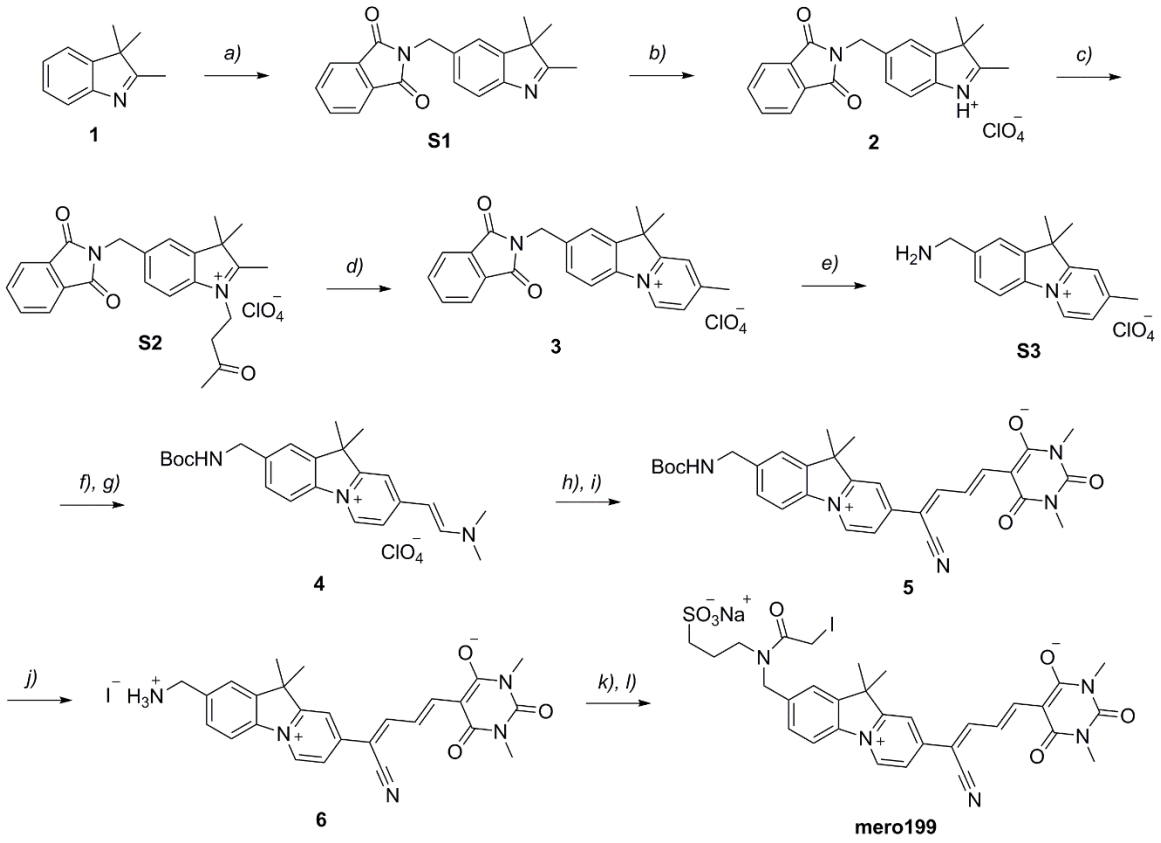

Key: a) H_2SO_4, 2-(hydroxymethyl)-1*H*-isoindole-1,3(2*H*)-dione; b) $HClO_4$, EtOH; c) methyl vinyl ketone; d) pyridine; e) $NH_2NH_2 .H_2O$; f) Boc_2O, Et_3N; g) $(CH_3O)_2CHN(CH_3)_2$, DBU; h) NH_2SO_3H; i) 5-((3)-methoxy-allylidene)-1,3-dimethyl-pyrimidine-2,4,6-trione, NaOAc; j) $(CH_3)_3SiI$, ACN; k) 1,3-propane sultone, NMP; l) $(ICH_2CO)_2O$, NMP.

Scheme S1. Full synthetic route to **mero199**.

2-((2,3,3-Trimethyl-3H-indol-5-yl)methyl)isoindoline-1,3-dione (S1). Sulfuric acid (167 mL) was added to a 500 mL round-bottom flask equipped with magnetic stir bar. The flask was cooled in an ice-water bath and 2,3,3-trimethyl-3*H*-indole (39.8 g, 250 mmol) was added dropwise over 45 min with stirring. The ice bath was removed and 2-(hydroxymethyl)-1*H*-isoindole-1,3(2*H*)-dione (112 g, 0.632 mol) was added to the reaction mixture at once. The flask was closed with a glass stopper and the stirring was continued for 120 h at room temp. The reaction mixture was added to a 2 L conical flask containing 1000 mL of ice. The flask was immersed in an ice-salt bath and an aqueous solution of NaOH (9.0 M) that had been chilled to 10 °C was slowly added to the reaction mixture until pH reached 7.0 with stirring at such a rate as to maintain the temperature of the reaction mixture below 20 °C. The precipitate was filtered, washed thoroughly with water, and dried open to air for 12 h. The crude product was placed in a 1 L conical flask and acetone (500 mL) was added. The mixture was stirred with heating to maintain a gentle boil for 10 min. The flask was cooled in an ice-water bath and the separated crystals were filtered, washed with acetone, and dried. Filtrates were combined, reduced in volume to about 100 mL and cooled at -10 °C overnight. The resulting crystals were filtered, washed with acetone, and dried. Isolated a combined total yield of 40.0 g (50%) pale brown solid. ^{1}H NMR (400 MHz, $CDCl_3$) δ 7.86 – 7.81 (m, 2H), 7.72 – 7.66 (m, 2H), 7.47 – 7.35 (m, 3H), 4.86 (s, 2H), 2.24 (s, 3H), 1.27 (s, 6H). ^{13}C NMR (100 MHz, $CDCl_3$) δ 188.8, 168.2, 153.7, 146.3, 134.2, 133.5, 132.4, 128.7, 123.5, 122.3, 120.0, 53.9, 41.9, 23.3, 15.6. MS-ESI *m/z* 319.2 ($[M + H]^+$ requires 319.1).

5-(1,3-Dioxo-1,3-dihydro-isoindol-2-ylmethyl)-2,3,3-trimethyl-3H-indolium perchlorate (2). Compound **S1** (5.16 g, 16.2 mmol) was placed in a 100 mL flask with magnetic stir bar. Ethanol (20.0 mL) was added, followed by addition of perchloric acid (1.42 mL, 16.5 mmol). The reaction mixture was stirred with heating under reflux for 30 min. The solution was then cooled to -10 °C for 3 h and the resulting crystals were filtered, washed with cold ethanol (1 X 25 mL), diethyl ether (2 x 25 mL), and dried to give 6.08 g (90%) brownish-red solid. ^{1}H NMR (400 MHz, DMSO-d_6) δ 7.99 – 7.79 (m, 4H), 7.67 (s, 1H), 7.55 (d, *J* = 8.0 Hz, 1H), 7.41 (d, *J* = 8.2 Hz, 1H), 4.86 (s, 2H), 2.58 (s, 3H), 1.42 (s, 6H). ^{13}C NMR (100 MHz, DMSO-d_6) δ 195.7, 167.7, 143.9, 142.3, 136.7, 134.6, 131.6, 127.5, 123.3, 122.1, 116.9, 53.8, 40.8, 22.0, 14.9. MS-ESI *m/z* 319.2 ($[M - ClO_4^-]^+$ requires 319.1).

5-(1,3-Dioxo-1,3-dihydro-isoindol-2-ylmethyl)-2,3,3-trimethyl-1-(3-oxo-butyl)-3H-indolium perchlorate (S2). Compound **2** (6.06 g, 15.7 mmol) was added to a 50 mL round-bottom flask equipped with magnetic stir. Methyl vinyl ketone (6.46 mL, 78.3 mmol) was added and the flask was heated to reflux for 15 min. The reaction mixture was concentrated and acetone (10 mL) was added to the residue. The flask was heated with stirring until the residue completely dissolved. The flask was then cooled to -10 °C for 3 h. The crystallized product was separated by filtration, washed with cold acetone (2 x 10 mL), ether (2 x 10 mL), and dried to give 4.77 g (62%) off-white solid. ^{1}H NMR (400 MHz, DMSO-d_6) δ 8.00 – 7.83 (m, 5H), 7.80 (s, 1H), 7.55 (d, *J* = 8.3 Hz, 1H), 4.90 (s, 2H), 4.54 (t, *J* = 6.2 Hz, 2H), 3.19 (t, *J* = 6.4 Hz, 2H), 2.82 (s, 3H), 2.12 (s, 3H), 1.49 (s, 6H).

2-(1,3-Dioxo-1,3-dihydro-isoindol-2-ylmethyl)-8,10,10-trimethyl-10H-pyrido[1,2-a]indolylium (3). Compound **S2** (4.72 g, 9.65 mmol) and pyridine (9.65 mL) were added to a 50 mL flask equipped with magnetic stir bar and the reaction mixture was heated to reflux for 1 h. The reaction mixture was concentrated and toluene (7.5 mL) was added to the semi-solid residue. The mixture was heated to reflux for 30 min. The flask was cooled and the toluene layer was decanted from the solid precipitate. Ethanol (7.5 mL) was added to the residue and the mixture was stirred under reflux for 10 min. The solid was filtered from the hot solution and

rinsed with ethanol. This process was repeated (1 X) and the isolated solid was dried under vacuum to give 1.26 g (28%) off-white solid. ^{1}H NMR (400 MHz, DMSO-d_6) δ 9.65 (d, *J* = 6.2 Hz, 1H), 8.42 (s, 1H), 8.30 (d, *J* = 8.2 Hz, 1H), 8.07 (d, *J* = 5.9 Hz, 1H), 7.95 – 7.85 (m, 5H), 7.64 (d, *J* = 8.0 Hz, 1H), 4.93 (s, 2H), 2.70 (s, 3H), 1.66 (s, 6H). ^{13}C NMR (100 MHz, DMSO-d_6) δ 168.2, 163.1, 159.5, 142.4, 140.3, 138.6, 135.1, 135.0, 132.2, 128.5, 127.1, 124.0, 123.7, 123.4, 115.4, 47.8, 41.2, 25.4, 22.4. MS-ESI *m/z* 369.3 ([M - ClO_4^-]$^+$ requires 369.2).

2-Aminomethyl-8,10,10-trimethyl-10H-pyrido[1,2-a]indolylium perchlorate (S3). Compound **3** (1.23 g, 2.62 mmol) was added to a 50 mL conical flask equipped with magnetic stir bar and 3:2 CH_2Cl_2/CH_3OH (15.0 mL). Stirring was started and hydrazine monohydrate (0.827 mL, 17.1 mmol) was added to the reaction mixture in bulk. Stirring was continued until all solids dissolved. The flask was closed with a stopper and let stand at room temperature overnight. After 16 h, the solid precipitate was filtered off and washed with 3:2 CH_2Cl_2-CH_3OH (15.0 mL). The combined filtrates were evaporated and the resulting solid was washed with 3:1 Et_2O/CH_3OH (1 X 10 mL), ether (1 X 10 mL), and dried to provide 0.872 g (98%) light brown solid. ^{1}H NMR (400 MHz, DMSO-d_6) δ 9.65 (d, *J* = 6.4 Hz, 1H), 8.44 (s, 1H), 8.28 (d, *J* = 8.4 Hz, 1H), 8.07 (d, *J* = 6.6 Hz, 1H), 7.85 (s, 1H), 7.65 (d, *J* = 8.3 Hz, 1H), 3.89 (s, 2H), 3.55 (bs, 2H), 2.71 (s, 3H), 1.67 (s, 6H). ^{13}C NMR (100 MHz, DMSO-d_6) δ 162.5, 158.6, 147.3, 141.4, 137.2, 134.4, 127.8, 126.6, 123.6, 122.5, 114.3, 47.2, 45.2, 25.1, 21.9. MS-ESI *m/z* 239.1 ([M - ClO_4^-]$^+$ requires 239.2).

2-(tert-Butoxycarbonylamino-methyl)-8-cyanomethyl-10,10-dimethyl-10H-pyrido[1,2-a]indolylium perchlorate (4). Compound **S3** (0.850 g, 2.51 mmol) was suspended in 3:1 CH_2Cl2/CH_3CN (16.0 mL) and triethylamine (0.525 mL, 3.76 mmol) was added. Di-*tert*-butyl dicarbonate (0.821 g, 3.76 mmol) was dissolved in CH_2Cl_2 (1.5 mL) and added to the reaction mixture. The flask was capped with a drying tube and allowed to stir for 24 h at room temp. The solvent was evaporated and the resulting crude brown solid was carried forward as intermediate. MS-ESI *m/z* 339.1 ([M - ClO_4^-]$^+$ requires 339.2).

The crude intermediate was diluted in dimethylformamide (2.20 mL). *N*,*N*-dimethylformamide dimethyl acetal (1.26 mL, 9.40 mmol) was added to the flask, followed by 1,8-diazabicyclo[5.4.0]undec-7-ene (3.7 µL, 0.025 mmol). The flask was heated to 100 °C for 30 min and cooled to room temp. The solvent was evaporated and the residue was recrystallized from methanol to give 0.847 g (68% from compound **S3**) green crystalline solid. ^{1}H NMR (400 MHz, DMSO-d_6) δ 8.84 (d, *J* = 5.9 Hz, 1H), 8.23 (d, *J* = 12.4 Hz, 1H), 7.93 (d, *J* = 7.3 Hz, 1H), 7.55 (s, 1H), 7.47 (s, 1H), 7.40 (d, *J* = 7.5 Hz, 2H), 5.47 (d, *J* = 12.4 Hz, 1H), 4.21 (s, 2H), 3.26 (s, 3H), 3.10 (s, 1H), 3.01 (s, 3H), 1.58 (s, 6H), 1.40 (s, 9H). ^{13}C NMR (DMSO-d_6, 75 MHz) *δ* 160.0, 155.8, 155.6, 153.1, 140.6, 140.0, 137.5, 131.5, 127.2, 122.2, 112.2, 93.9, 78.0, 45.9, 45.0, 43.3, 37.1, 28.2, 26.3. MS-ESI *m/z* 394.2 ([M - ClO_4^-]$^+$ requires 394.3).

{8-[1-Cyano-4-(1,3-dimethyl-2,4,6-trioxo-tetrahydro-pyrimidin-5-ylidene)-but-2-enylidene]-10,10-dimethyl-8,10-dihydro-pyrido[1,2-a]indol-2-ylmethyl}-carbamic acid tert-butyl ester (5). Compound **4** (0.795 g, 1.61 mmol) was suspended in 1:1 MeOH/H2O (23.0 mL). Stirring was started and hydroxylamine-O-sulfonic acid (0.780 g, 6.90 mmol) was added to the flask in bulk. The flask was capped with a septum with needle vent open to air. Stirring was continued for a total of 24 h at room temp. Solid sodium bicarbonate was added to the reaction mixture to adjust pH to 7.0. The reaction mixture was concentrated under vacuum to remove methanol. The product deposited on the inner wall of the flask as a dark brown tar. The remaining aqueous solution was decanted and the deposited tar was washed with water (2 x 20 mL) and ether (1 x 20 mL) and dried under vacuum. The isolated semi-solid was carried forward as intermediate. MS-ESI *m/z* 364.1 ([M - ClO_4^-]$^+$ requires 364.2).

5-(3-Methoxy-allylidene)-1,3-dimethyl-pyrimidine-2,4,6-trione (0.245 g, 1.09 mmol) and sodium acetate (0.149 g, 1.82 mmol) were added to the crude intermediate (0.422 g, 0.910 mmol), followed by addition of 1:1 CH_2Cl_2/MeOH (10.0 mL). The reaction was allowed to reflux for 30 min. The dark blue solution was cooled to room temperature and concentrated with silica (2.5 g). The silica cake was eluted on a 24 g silica column with 0 – 5% MeOH in CH_2Cl_2 over 17 min. Major product peaks were combined and concentrated to give 0.249 g (29% from compound **4**) dark blue solid. ^{1}H NMR (400 MHz, DMSO-d_6) δ 9.01 (d, J = 7.2 Hz, 1H), 8.37 (d, J = 13.0 Hz, 1H), 8.06 (bs, 1H), 8.01 (s, 1H), 7.98 (t, J = 4.1 Hz, 1H), 7.72 (t, J = 13.1 Hz, 1H), 7.59 – 7.50 (m, 2H), 7.47 (t, J = 5.8 Hz, 1H), 7.40 (d, J = 8.4 Hz, 1H), 4.22 (d, J = 5.8 Hz, 2H), 3.17 (s, 3H), 3.12 (s, 3H), 1.64 (s, 6H), 1.41 (s, 9H). ^{13}C NMR (100 MHz, DMSO-d_6) δ 163.2, 162.2, 160.9, 156.2, 155.0, 154.4, 152.0, 151.8, 141.8, 141.1, 137.8, 132.9, 127.8, 122.6, 118.6, 116.6, 113.2, 111.5, 100.7, 88.7, 79.6, 78.5, 46.9, 43.8, 28.7, 28.2, 27.5, 26.5. MS-ESI *m/z* 578.3 ([M + Na]$^+$ requires 578.2).

8-[1-Cyano-4-(1,3-dimethyl-2,4,6-trioxo-tetrahydro-pyrimidin-5-ylidene)-but-2-enylidene]-10,10-dimethyl-8,10-dihydro-pyrido[1,2-a]indol-2-ylmethyl-ammonium iodide (6). Compound **5** (0.164 g, 0.295 mmol) was placed in a 25 mL round-bottom flask equipped with magnetic stir bar. The flask was closed with a rubber septum, evacuated, and flushed with argon. Acetonitrile (1.64 mL) was added, followed by addition of iodotrimethylsilane (53 µL, 0.369 mmol). The reaction mixture was stirred at room temp for 30 min. Methanol (0.5 mL) was added and the reaction mixture was concentrated. The precipitated product was filtered and washed with acetonitrile. The product was suspended in CH_2Cl_2 (2.0 mL) and the mixture was heated to reflux for 10 min. The mixture was filtered while still hot, washed with DCM, and dried under vacuum. The product was isolated as 0.150 g (87%) dark blue solid. ^{1}H NMR (400 MHz, DMSO-d_6) δ 9.03 (d, J = 7.2 Hz, 1H), 8.39 (d, J = 13.0 Hz, 1H), 8.19 (bs, 3H), 8.09 (d, J = 8.4 Hz, 1H), 8.02 (d, J = 13.2 Hz, 1H), 7.81 (s, 1H), 7.73 (t, J = 13.1 Hz, 1H), 7.63 (d, J = 8.2 Hz, 1H), 7.55 (bs, 1H), 4.15 (q, J = 5.6 Hz, 2H), 3.17 (s, 3H), 3.13 (s, 3H), 1.66 (s, 6H). ^{13}C NMR (100 MHz, DMSO-d_6) δ 162.7, 161.7, 160.3, 154.4, 154.2, 151.6, 151.5, 140.7, 138.6, 134.4, 132.4, 129.5, 124.5, 118.1, 116.4, 113.0, 110.8, 100.8, 88.2, 46.4, 42.1, 27.8, 27.1, 26.1. MS-ESI *m/z* 456.5 ([M - I$^-$]$^+$ requires 456.2).

N-ethyl-N-isopropylpropan-2-aminium 3-(N-((8-((1Z,3E)-1-cyano-4-(1,3-dimethyl-6-oxido-2,4-dioxo-1,2,3,4-tetrahydropyrimidin-5-yl)buta-1,3-dienyl)-10,10-dimethyl-10H-pyrido[1,2-a]indolium-2-yl)methyl)-2-iodoacetamido)propane-1-sulfonate (mero199). Compound **6** (135 mg, 1.71 mmol) and NaOAc (37.9 mg, 0.462 mmol) were added to a 25 mL round-bottom flask with magnetic stir bar. The flask was sealed with a rubber septum, evacuated and argon flushed. *N*-Methyl-2-pyrrolidone (2.7 mL) was added, followed by addition of 1,3-propane sultone (42.4 mg, 0.347 mmol) as the solution in 0.675 mL NMP. The septum was replaced with a drying tube and the reaction mixture was allowed to stir at room temp for 48 h. The reaction mixture was used in the next step as intermediate. MS-ESI *m/z* 578.3 ([M + Na]$^+$ requires 578.2).

To the intermediate mixture was added a solution of iodoacetic anhydride (178 mg, 2.0 mmol) in *N*-methyl-2-pyrrolidinone (1.25 mL), followed by the addition of a solution of *N*,*N*-diisopropylethylamine (177 µL, 1.02 mmol) in *N*-methyl-2-pyrrolidinone (0.25 mL). The reaction mixture was stirred at room temperature for 30 min and then Et_2O (25 mL) was added to the flask to precipitate product. The purple solid was filtered, re-suspended in 1:1 MeOH-acetone (12.5 mL) and concentrated with silica gel (1.1 g). The silica cake was eluted on a silica column (24 g) with 0 – 15% MeOH in acetone. Main product containing fractions were combined and concentrated to near dryness and Et_2O (25 mL) was added. The mixture was filtered and the isolated precipitate was dried under vacuum. The crude product was dissolved in 4:1 water-acetonitrile, filtered through a nylon filter (0.45 µM) and submitted to preparative HPLC. Main

product containing fractions were combined, concentrated, and lyophilized. The product was isolated as 23 mg (14%, from compound **6**) dark blue solid. HRMS *m/z* 744.0992 ([M - Na^+]$^-$ requires 744.0994.

Spectroscopic Data for New Compounds

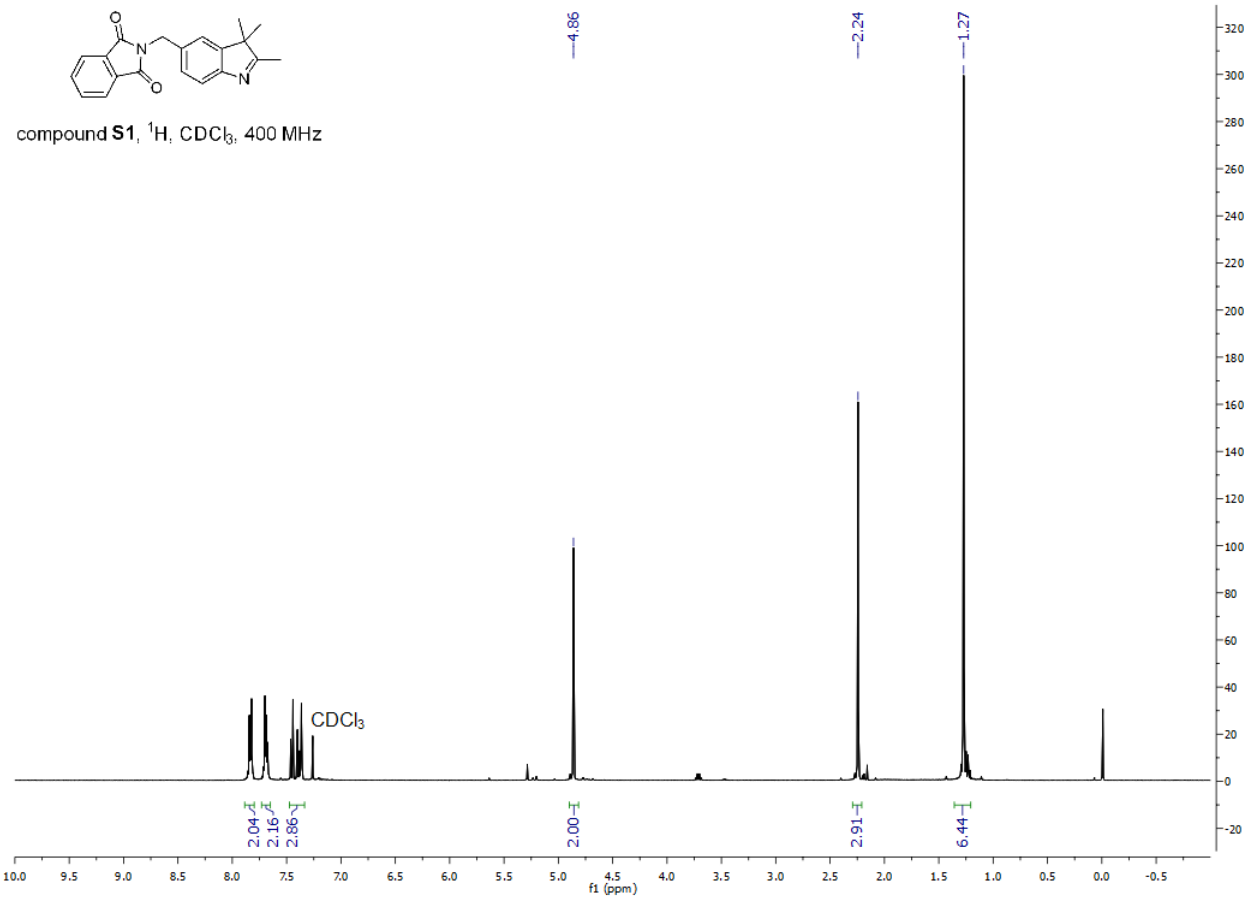

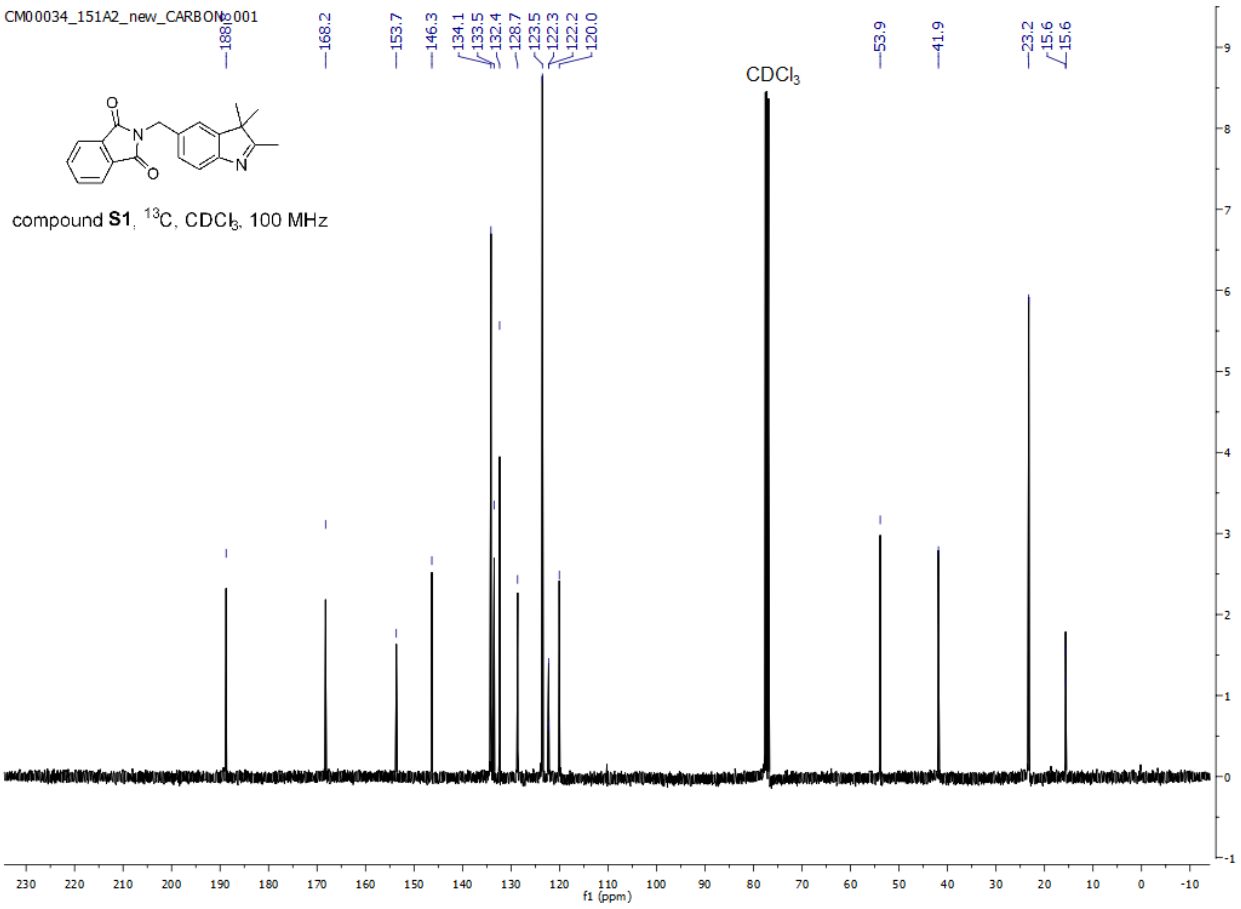

Compound **S1** LCMS:

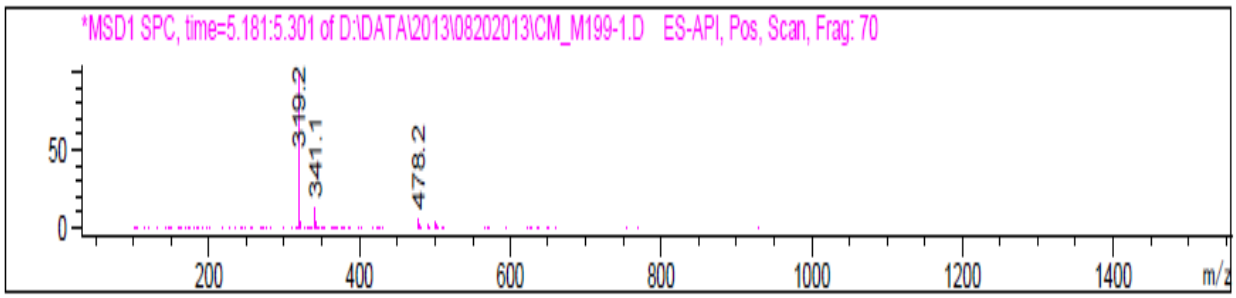

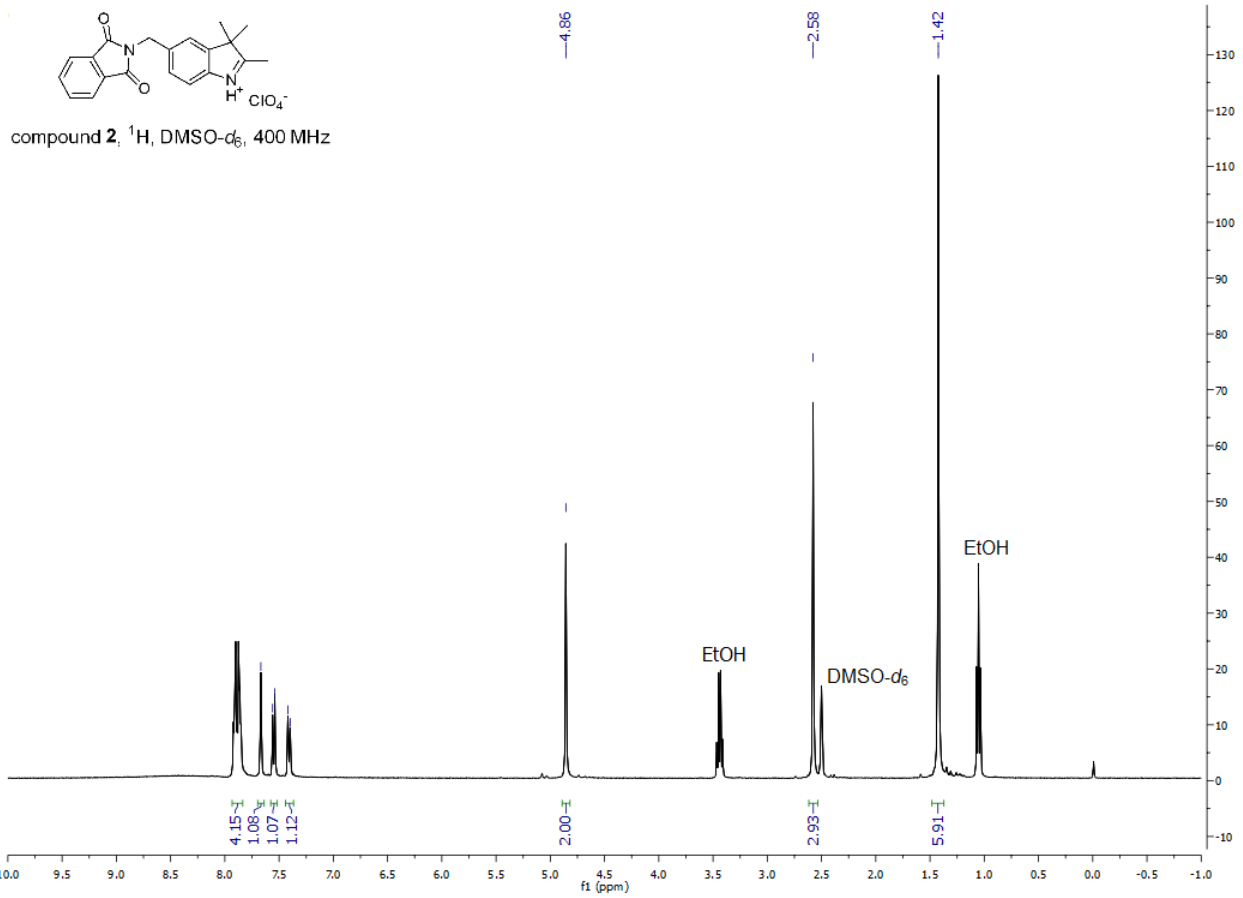
compound 2, 1H, DMSO-d6, 400 MHz
4.86
2.58
1.42
EtOH
DMSO-d6
EtOH
4.15
1.08
1.07
1.12
2.00
2.93
5.91
f1 (ppm)

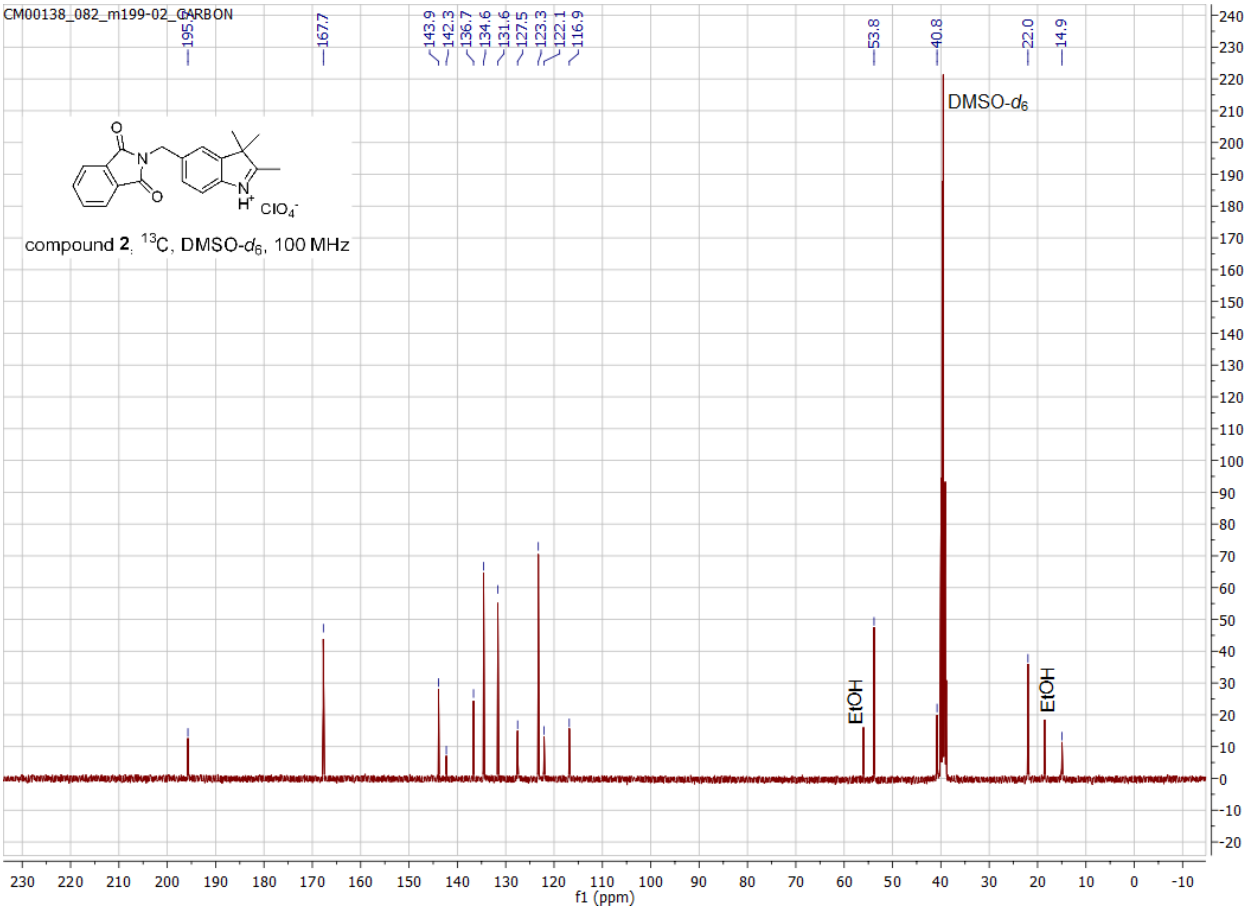

Compound **2** LCMS:

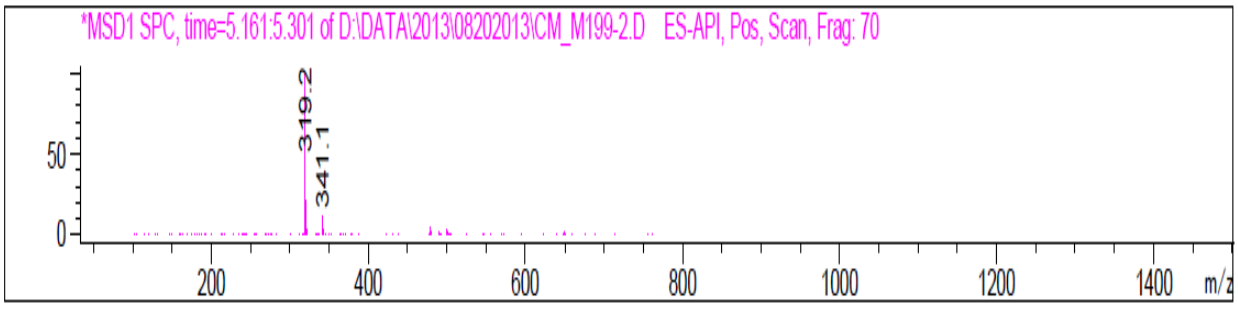

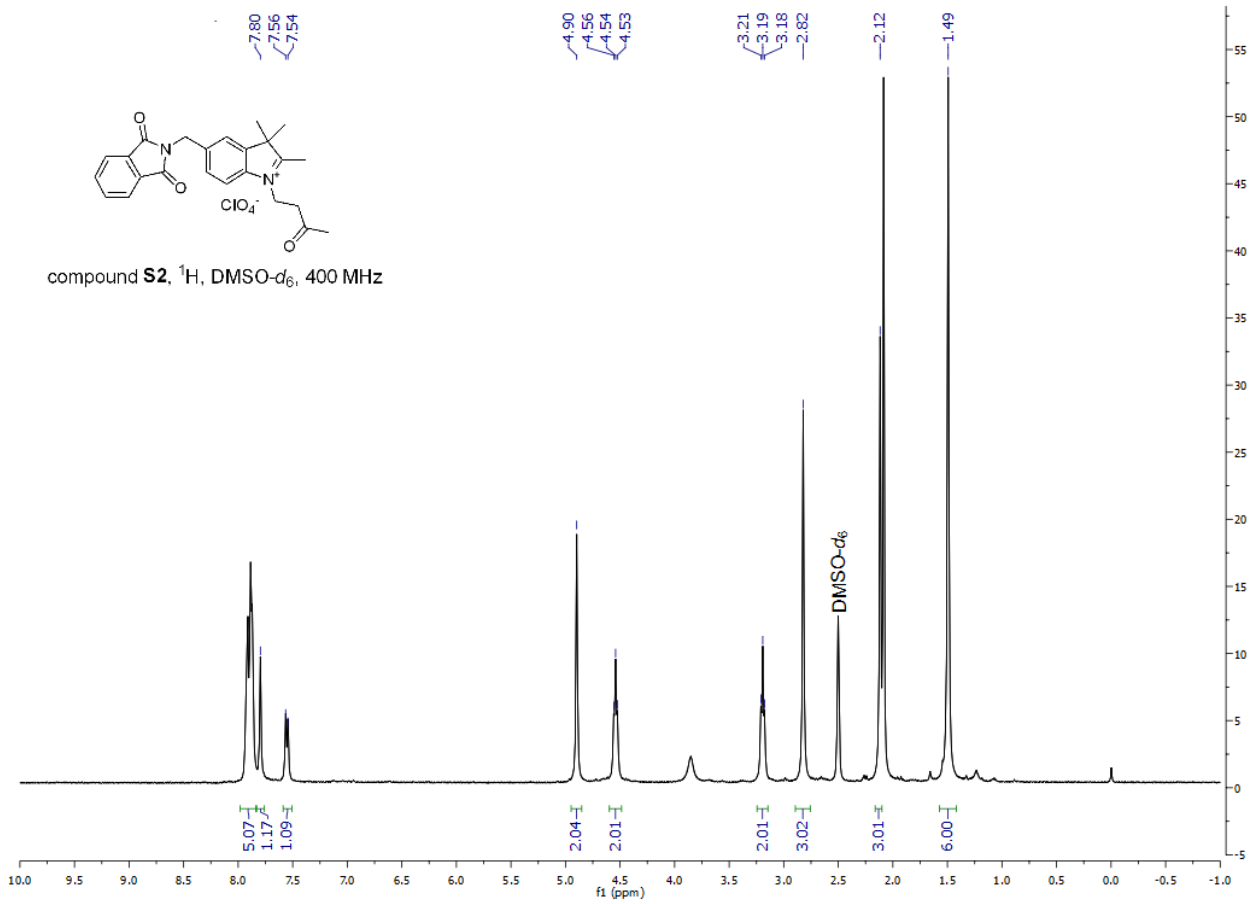

compound **S2**, ^{1}H, DMSO-d_6, 400 MHz

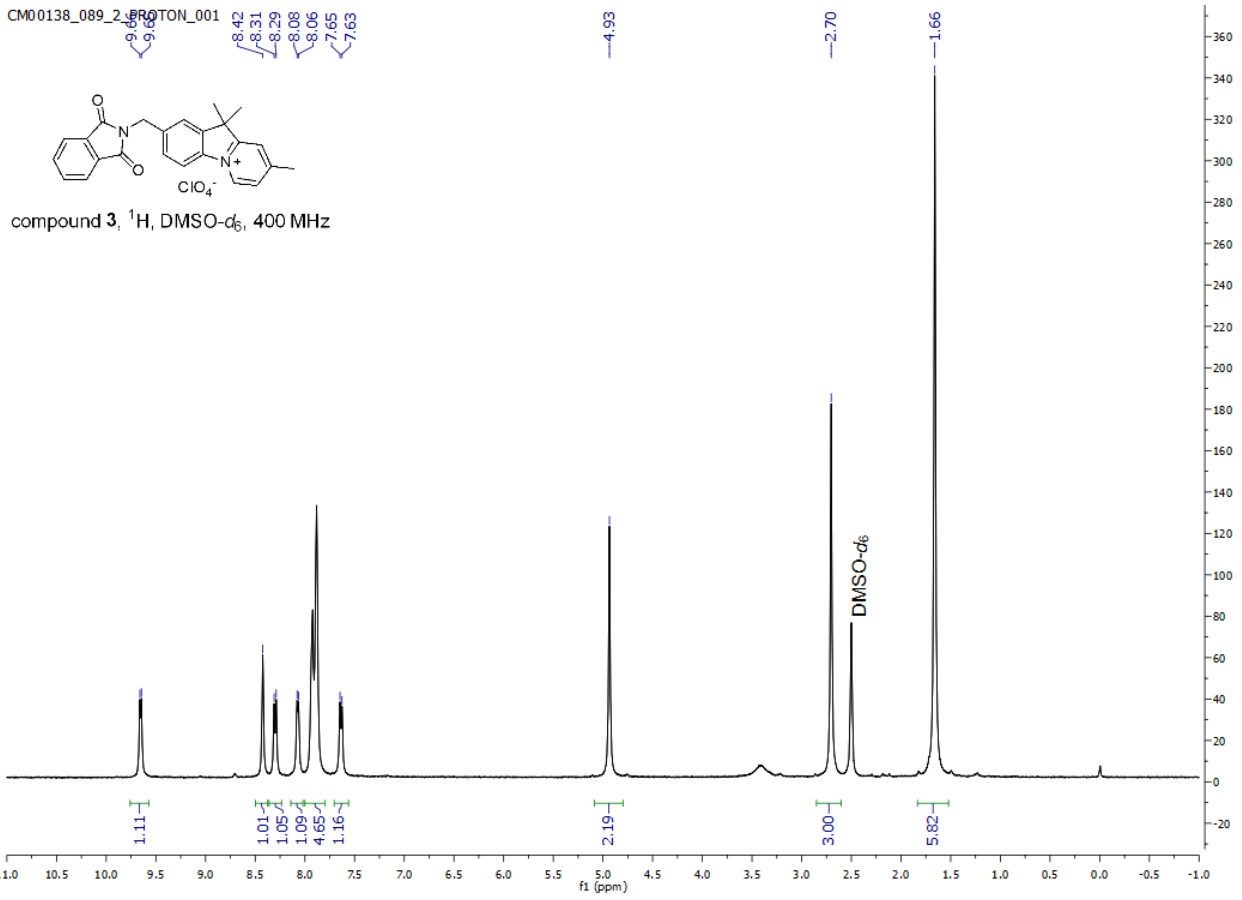

compound **3**, ^{1}H, DMSO-d_6, 400 MHz

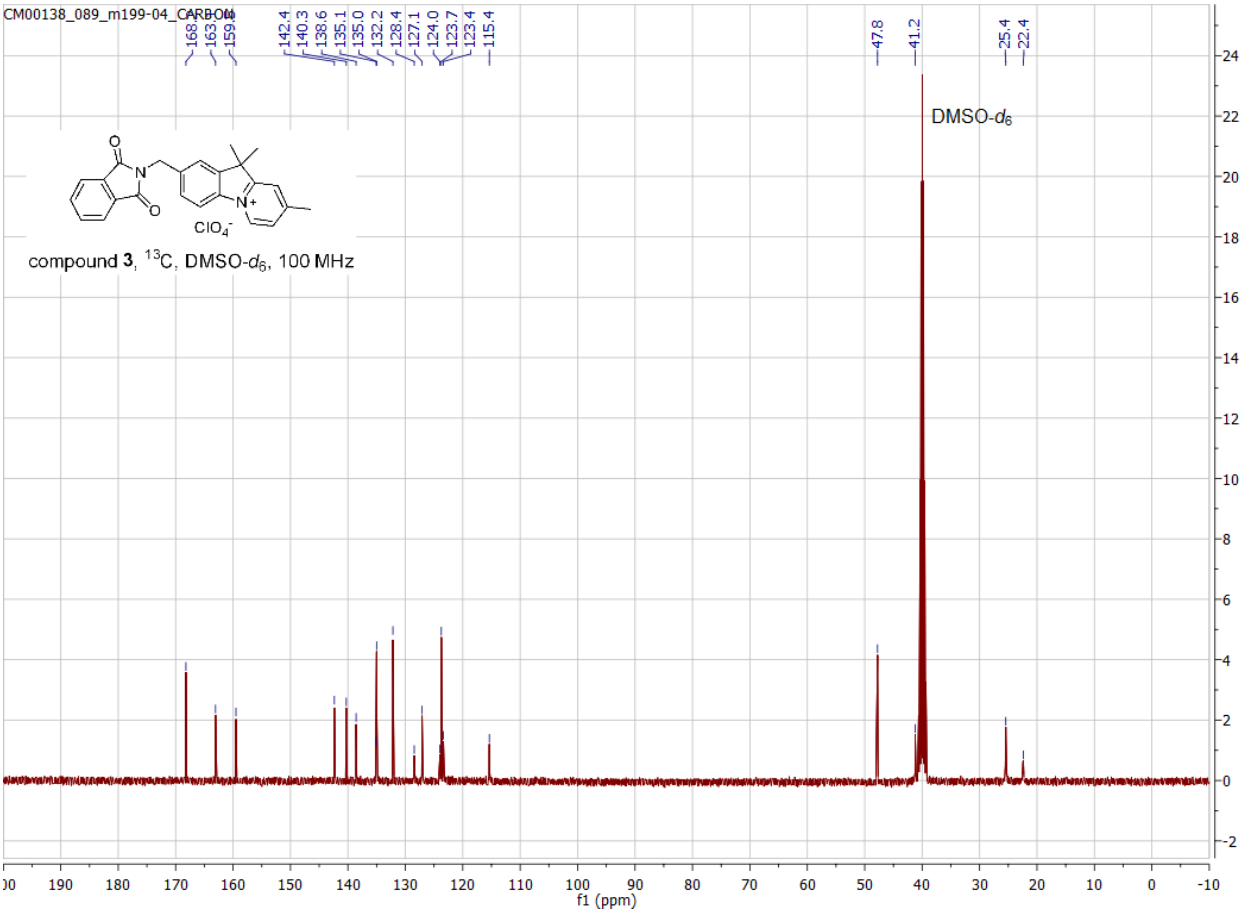
CM00138_089_m199-04_CARBON
168.1
163.0
159.8
142.4
140.3
138.6
135.1
135.0
132.2
128.4
127.1
124.0
123.7
123.4
115.4
47.8
41.2
25.4
22.4
DMSO-d_6
ClO_4^-
compound **3**, ^{13}C, DMSO-d_6, 100 MHz
f1 (ppm)

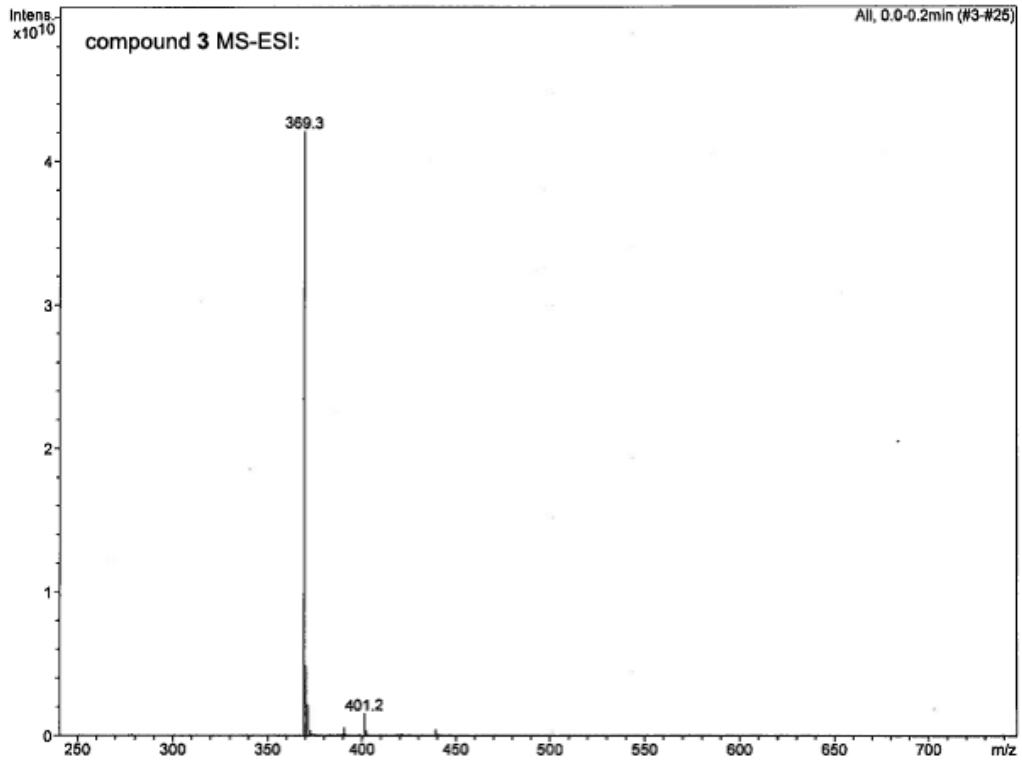
Intens.
x10^10
All, 0.0-0.2min (#3-#25)
compound **3** MS-ESI:
369.3
401.2
m/z

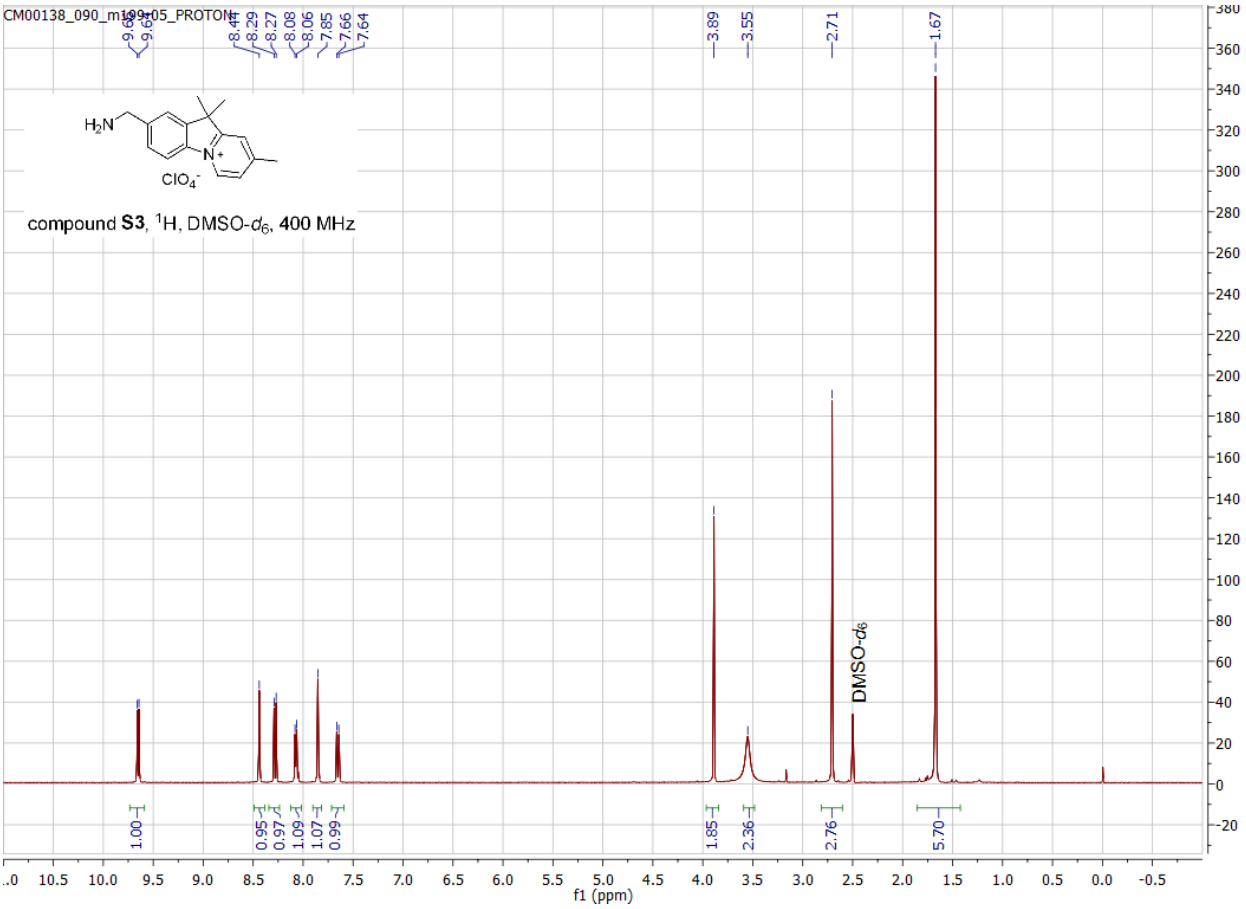
CM00138_090_m199-05_PROTON
9.68
9.65
8.44
8.29
8.27
8.08
8.06
7.85
7.66
7.64
3.89
3.55
2.71
1.67
H2N
N+
ClO4-
compound S3, 1H, DMSO-d6, 400 MHz
DMSO-d6
1.00
0.95
0.97
1.09
1.07
0.99
1.85
2.36
2.76
5.70
f1 (ppm)

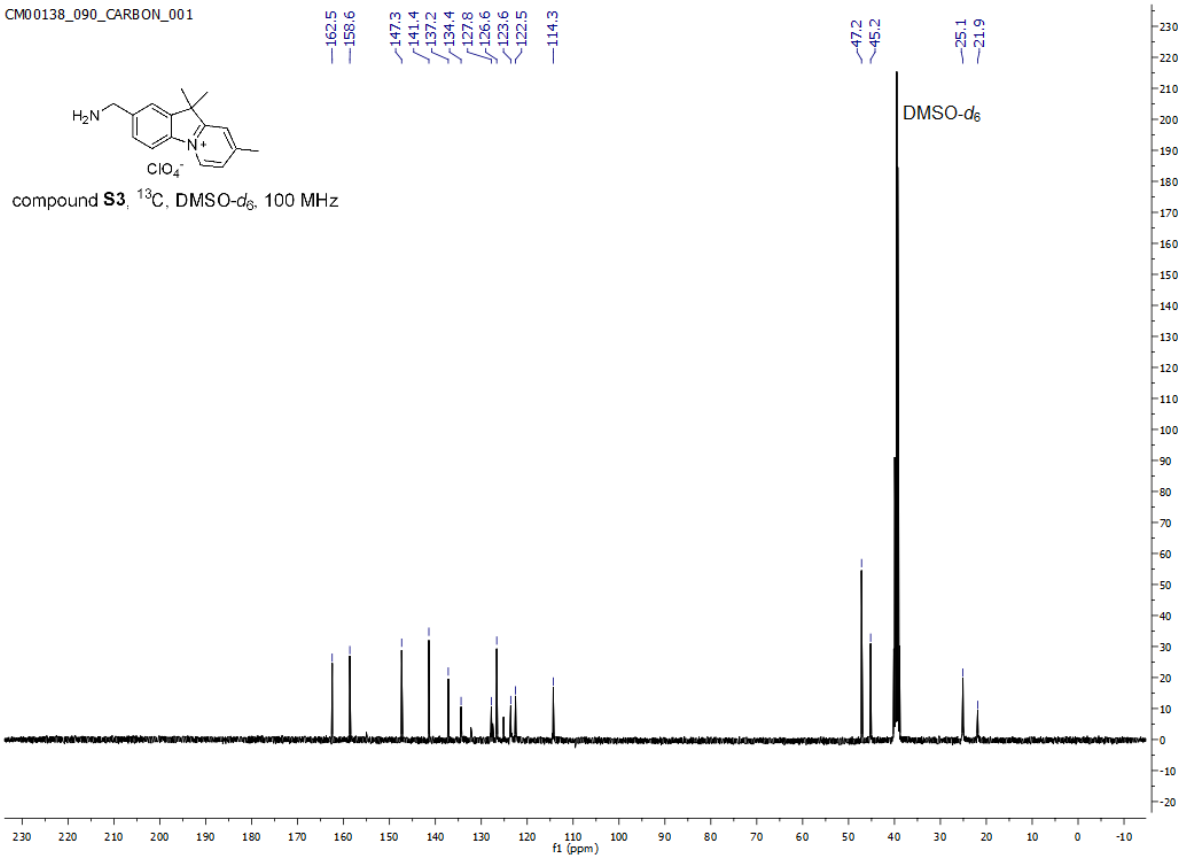
CM00138_090_CARBON_001
162.5
158.6
147.3
141.4
137.2
134.4
127.8
126.6
123.6
122.5
114.3
47.2
45.2
25.1
21.9
DMSO-d_6
H_2N
ClO_4^-
compound **S3**, ^{13}C, DMSO-d_6, 100 MHz
f1 (ppm)

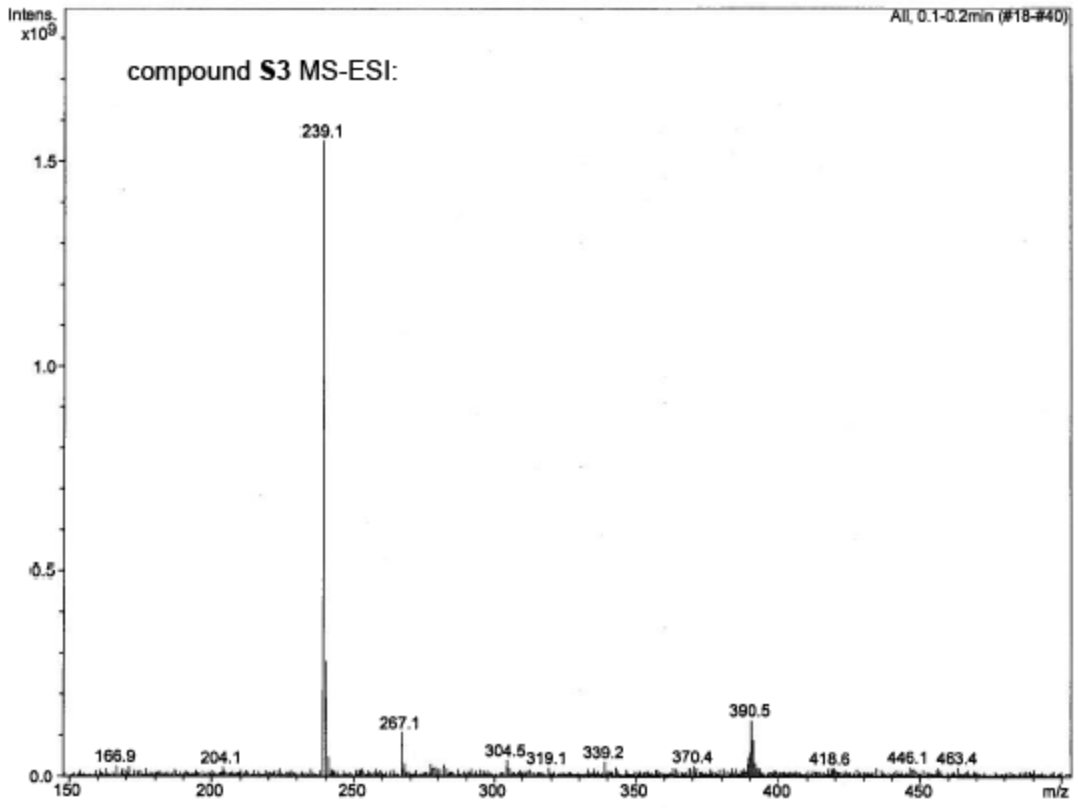
Intens.
x10^9
All, 0.1-0.2min (#18-#40)
compound **S3** MS-ESI:
239.1
267.1
390.5
166.9
204.1
304.5
319.1
339.2
370.4
418.6
446.1
463.4
m/z

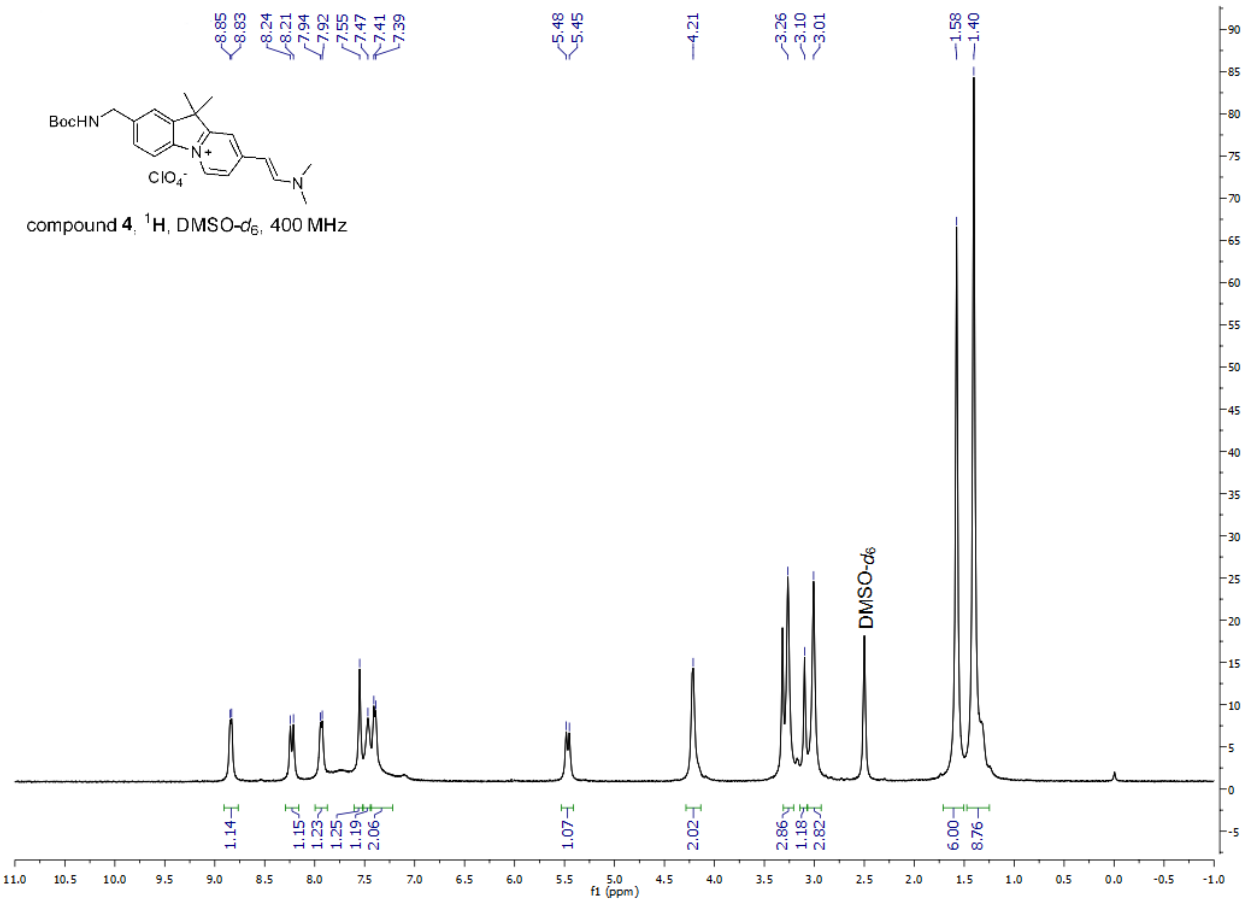
8.85
8.83
8.24
8.21
7.94
7.92
7.55
7.47
7.41
7.39
5.48
5.45
4.21
3.26
3.10
3.01
1.58
1.40
BocHN
N+
ClO4-
N
compound 4, 1H, DMSO-d6, 400 MHz
DMSO-d6
1.14
1.15
1.23
1.25
1.19
2.06
1.07
2.02
2.86
1.18
2.82
6.00
8.76
f1 (ppm)

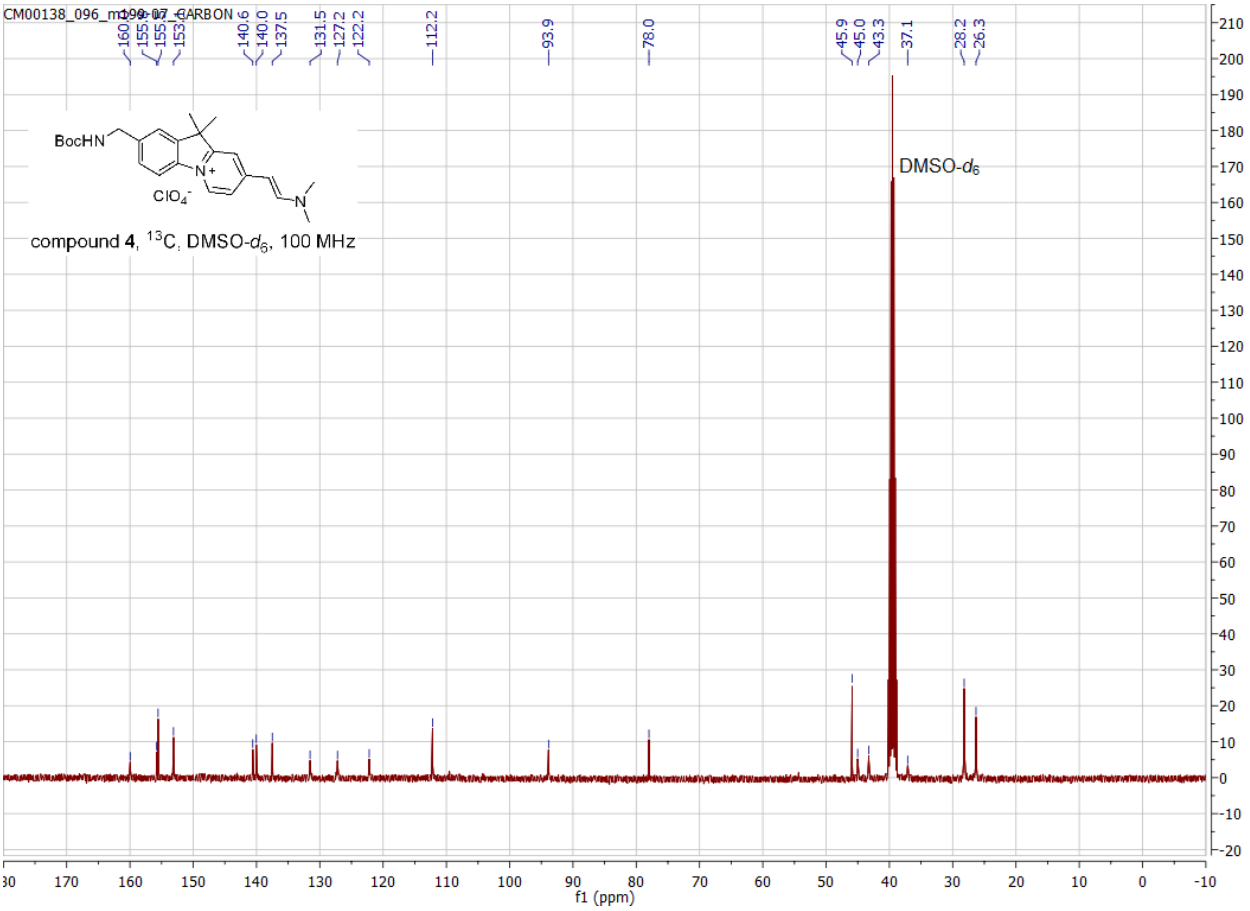
CM00138_096_m199_07_CARBON
160.0
155.4
155.1
153.1
140.6
140.0
137.5
131.5
127.2
122.2
112.2
93.9
78.0
45.9
45.0
43.3
37.1
28.2
26.3
DMSO-d_6
BocHN
N+
ClO_4^-
N
compound **4**, ^{13}C, DMSO-d_6, 100 MHz
f1 (ppm)

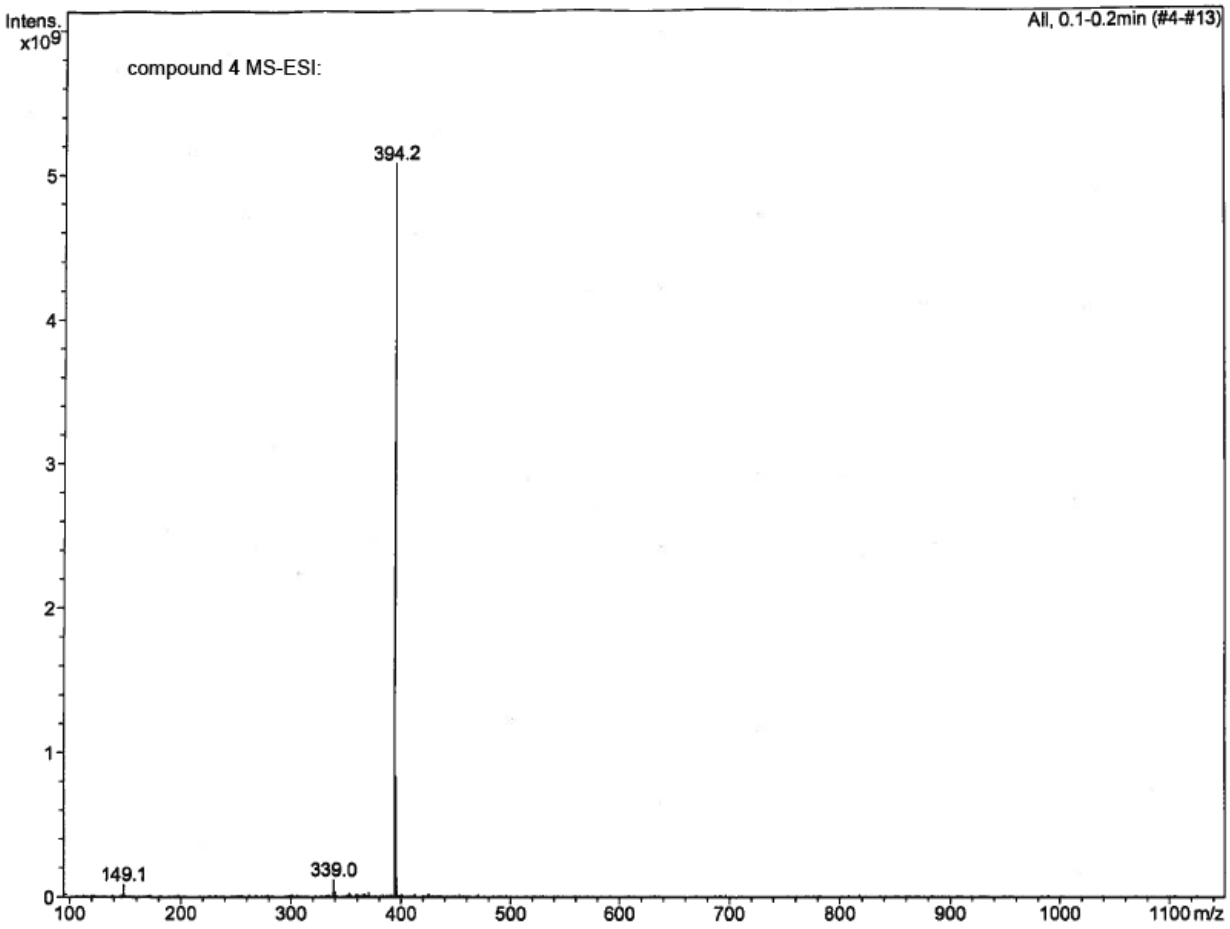
Intens.
x10^9
All, 0.1-0.2min (#4-#13)
compound 4 MS-ESI:
394.2
149.1
339.0
m/z

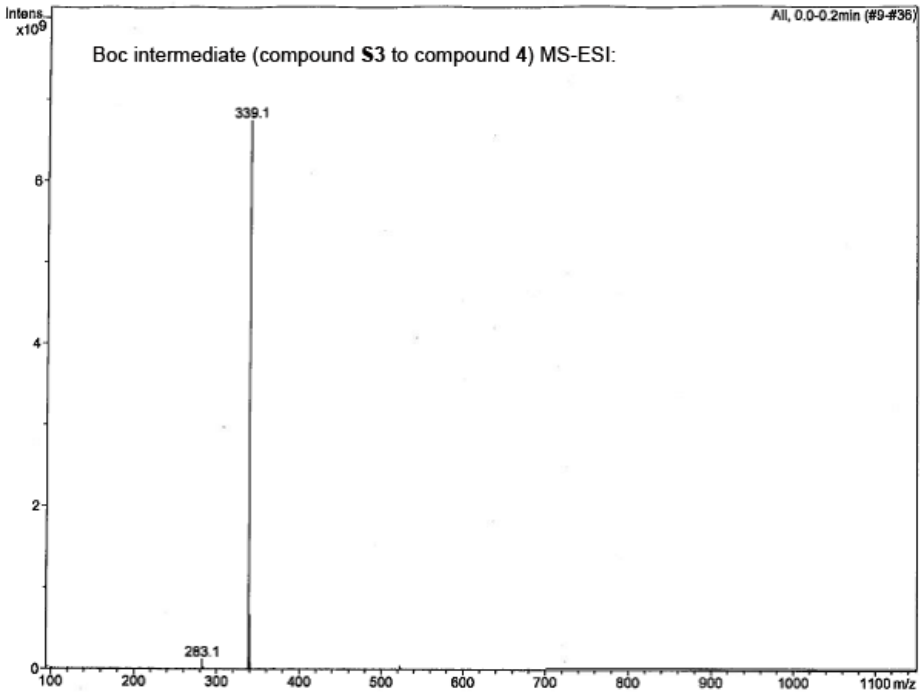
Intens.
x10^9
All, 0.0-0.2min (#9-#36)
Boc intermediate (compound S3 to compound 4) MS-ESI:
339.1
283.1
m/z

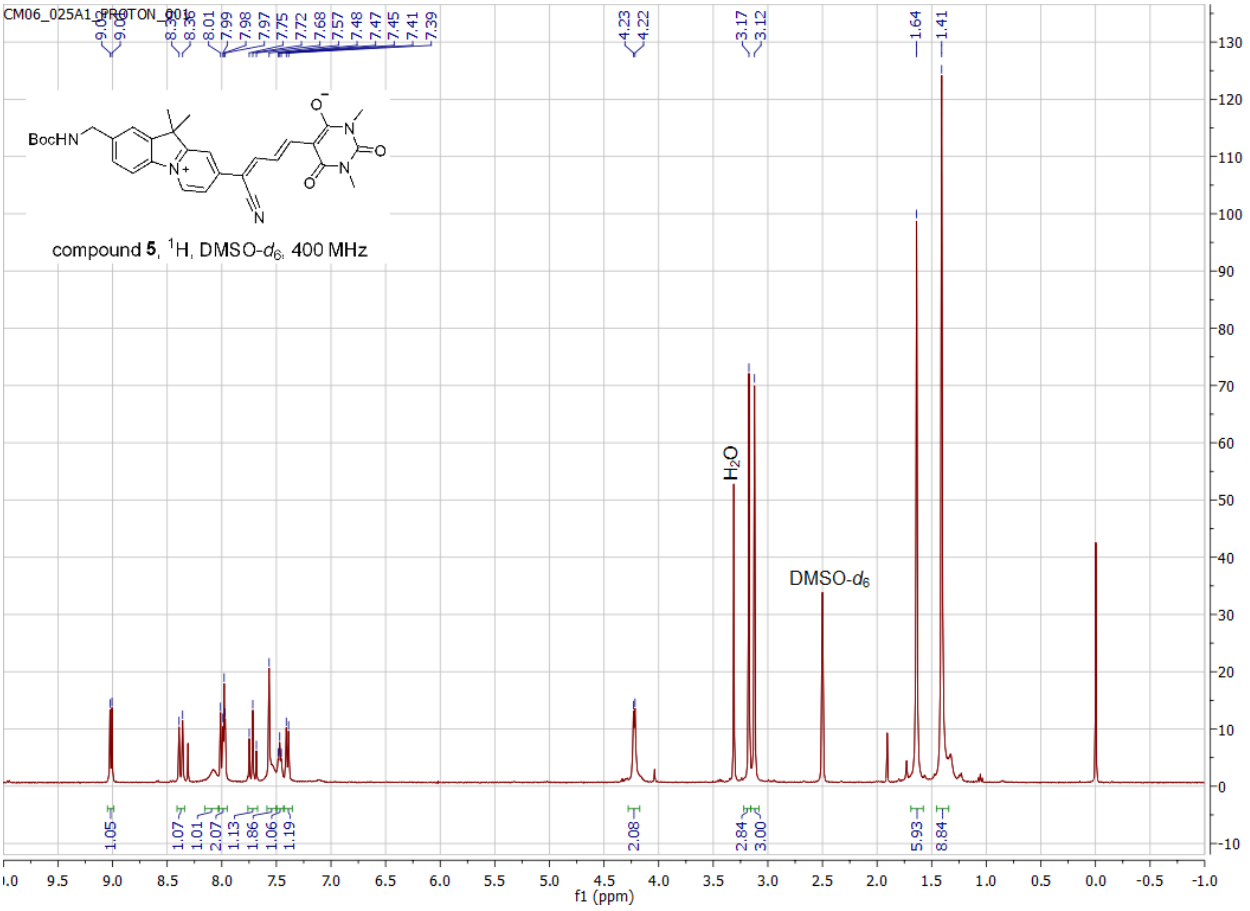
CM06_025A1_PROTON_001
BocHN
compound 5, 1H, DMSO-d6, 400 MHz
H2O
DMSO-d6
f1 (ppm)

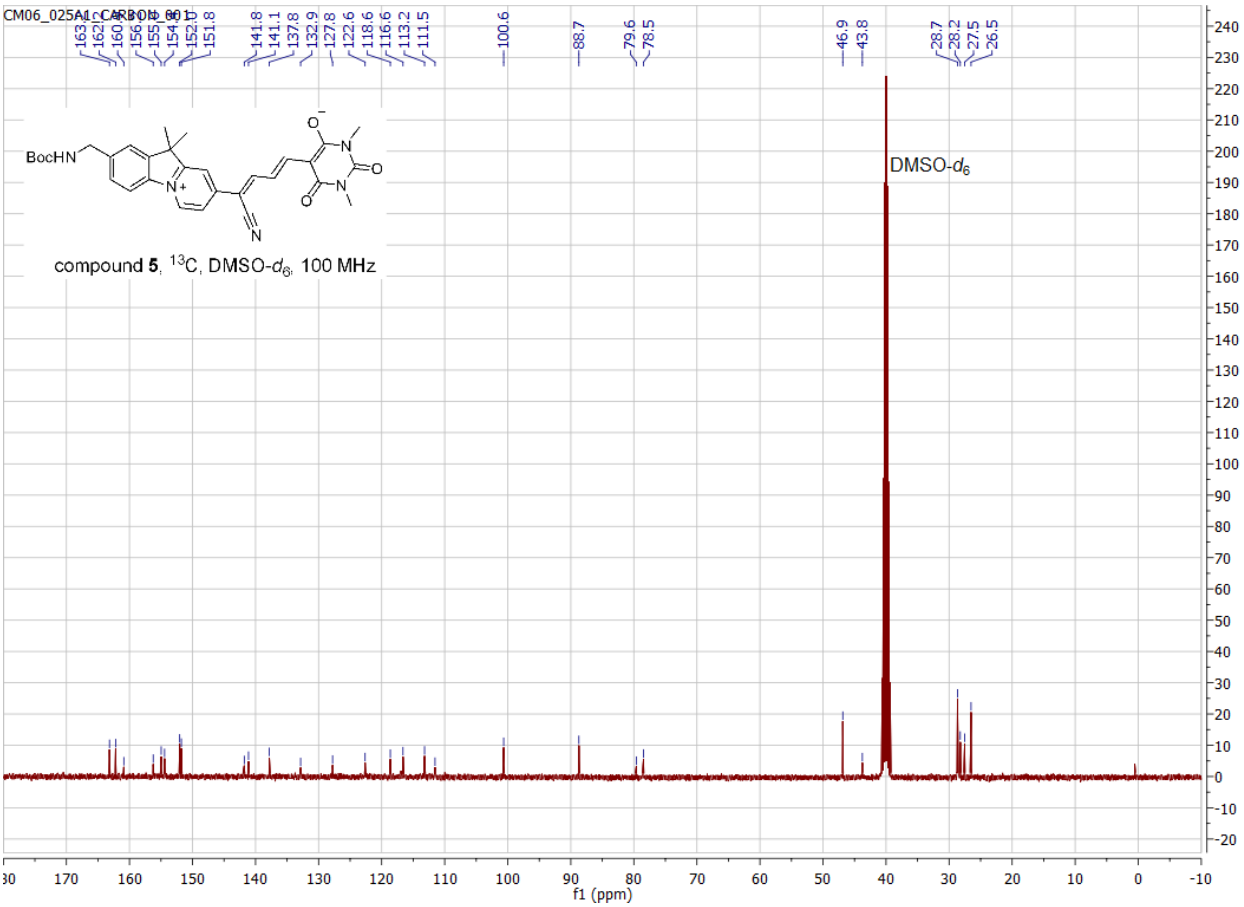
CM06_025A1_CARBON_601
163.1
162.1
160.6
156.1
155.1
154.1
152.0
151.8
141.8
141.1
137.8
132.9
127.8
122.6
118.6
116.6
113.2
111.5
100.6
88.7
79.6
78.5
46.9
43.8
28.7
28.2
27.5
26.5
DMSO-d_6
BocHN
compound **5**, ^{13}C, DMSO-d_6, 100 MHz
f1 (ppm)

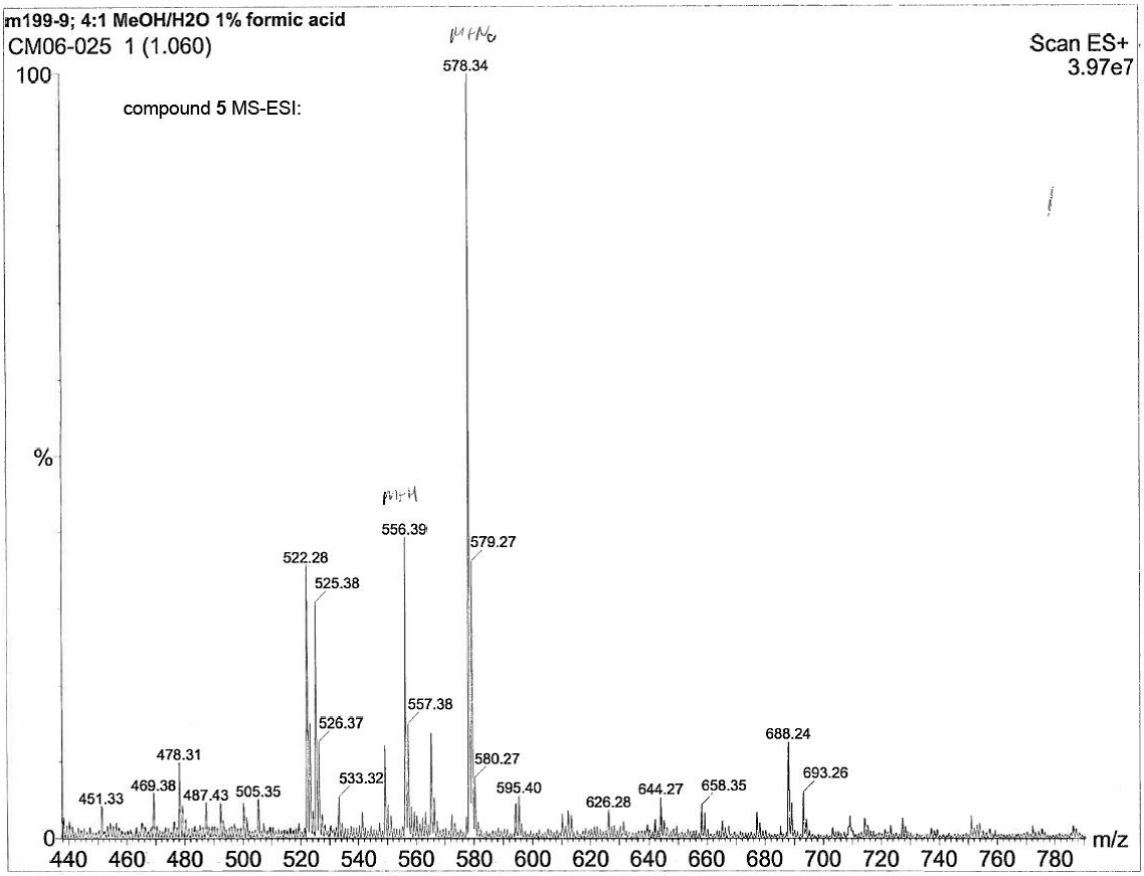
m199-9; 4:1 MeOH/H2O 1% formic acid
CM06-025 1 (1.060)
Scan ES+
3.97e7
100
%
0
compound 5 MS-ESI:
578.34
556.39
579.27
522.28
525.38
557.38
526.37
688.24
478.31
580.27
693.26
533.32
469.38
595.40
644.27
658.35
451.33
487.43
505.35
626.28
440 460 480 500 520 540 560 580 600 620 640 660 680 700 720 740 760 780
m/z

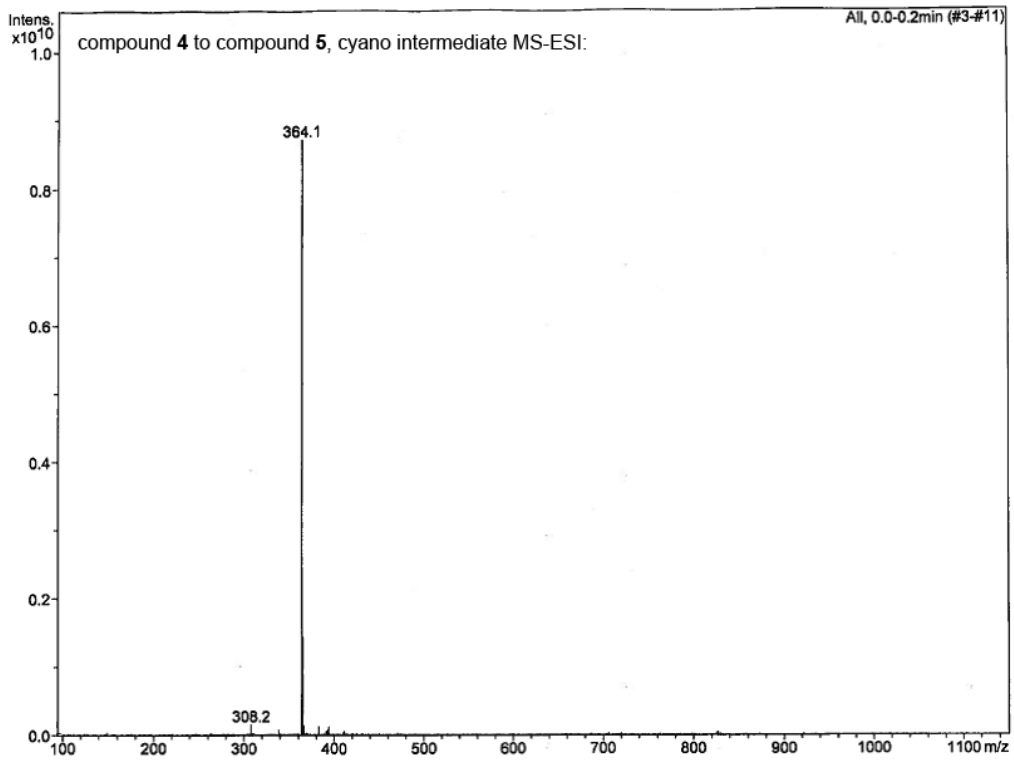
Intens.
x10^10
1.0
0.8
0.6
0.4
0.2
0.0
All, 0.0-0.2min (#3-#11)
compound 4 to compound 5, cyano intermediate MS-ESI:
364.1
308.2
100 200 300 400 500 600 700 800 900 1000 1100 m/z

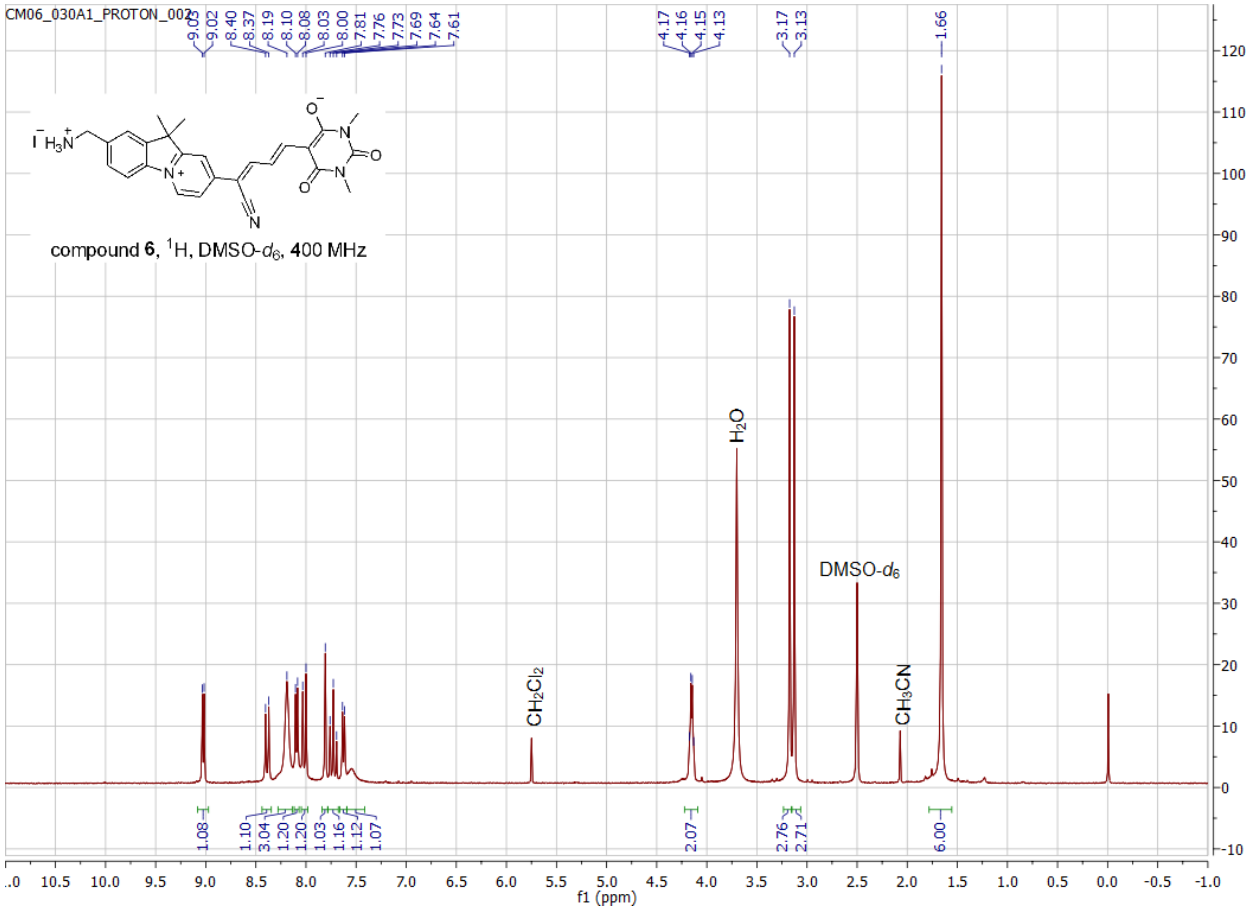
CM06_030A1_PROTON_002
compound 6, 1H, DMSO-d6, 400 MHz
CH2Cl2
H2O
DMSO-d6
CH3CN
f1 (ppm)

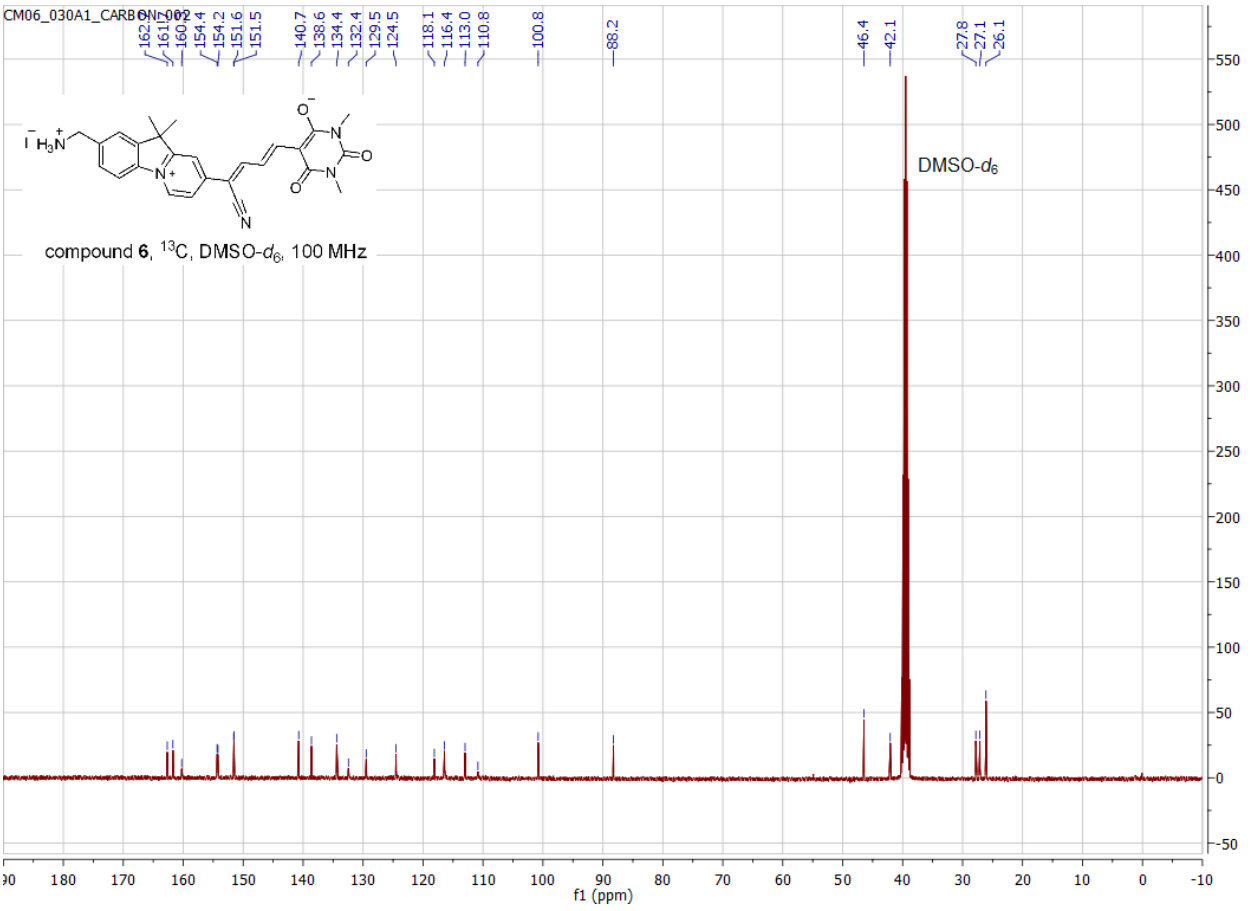
CM06_030A1_CARBON-002
162.2
161.2
160.2
154.4
154.2
151.6
151.5
140.7
138.6
134.4
132.4
129.5
124.5
118.1
116.4
113.0
110.8
100.8
88.2
46.4
42.1
27.8
27.1
26.1
DMSO-d_6
compound **6**, ^{13}C, DMSO-d_6, 100 MHz
f1 (ppm)

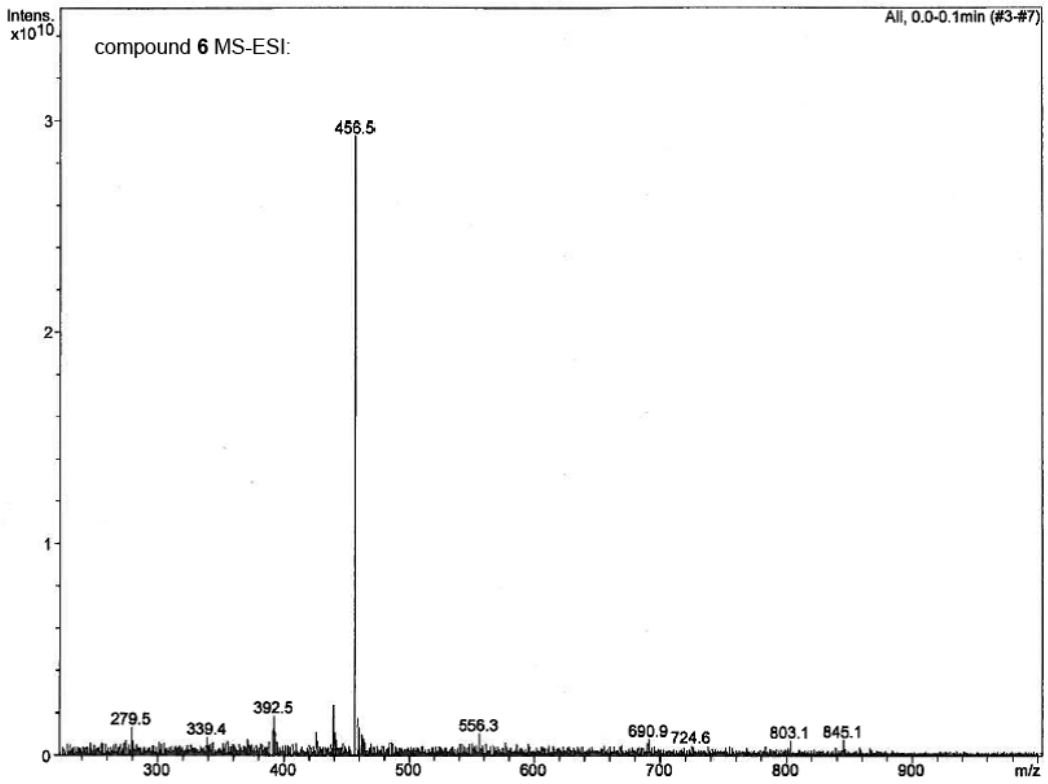
Intens.
x10^10
All, 0.0-0.1min (#3-#7)
compound **6** MS-ESI:
456.5
279.5
339.4
392.5
556.3
690.9
724.6
803.1
845.1
m/z

Mero199 HPLC:

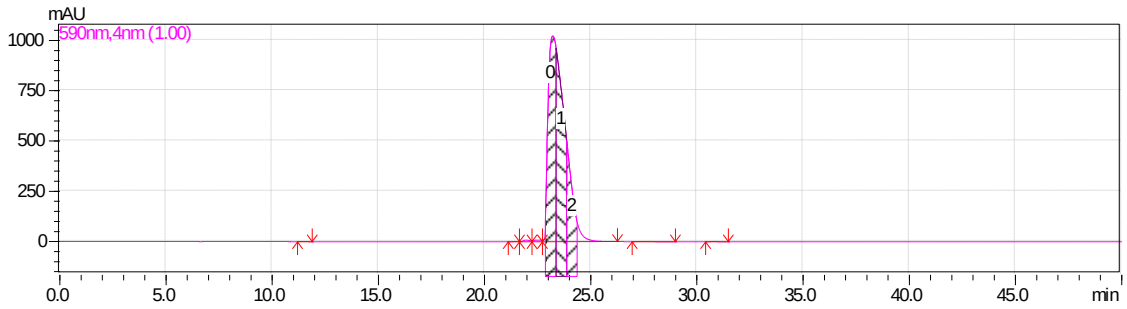

Peak#	Ret. Time	Area	Height	Peak Start	Peak End	Area%
1	21.952	179025	8498	21.643	22.229	0.3130
2	22.475	206472	8298	22.229	22.720	0.3610
3	23.207	56809942	1023518	22.720	26.261	99.3260

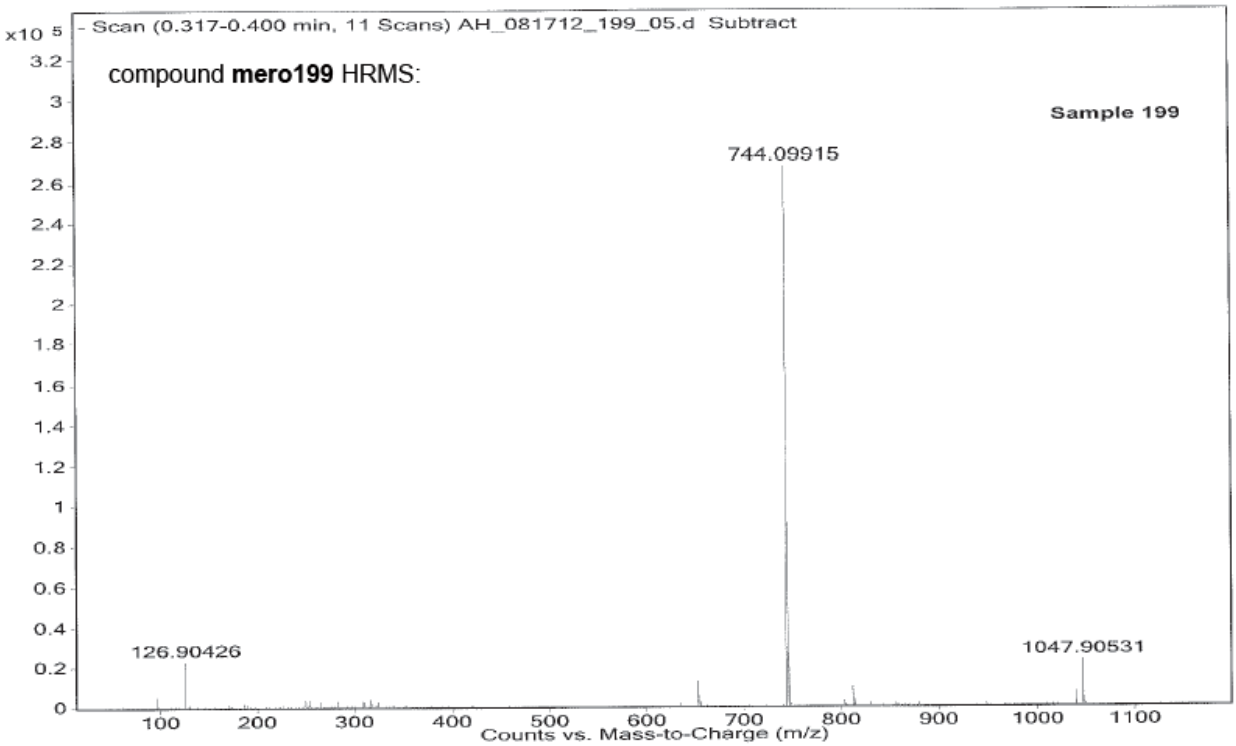

References

(1) Machacek, M.; Hodgson, L.; Welch, C.; Elliott, H.; Pertz, O.; Nalbant, P.; Abell, A.; Johnson, G. L.; Hahn, K. M.; Danuser, G. *Nature* **2009**, *461*, 99.
(2) Markwardt, M. L.; Kremers, G. J.; Kraft, C. A.; Ray, K.; Cranfill, P. J. C.; Wilson, K. A.; Day, R. N.; Wachter, R. M.; Davidson, M. W.; Rizzo, M. A. *Plos One* **2011**, *6*, e17896.
(3) Kim, J. H.; Lee, S. R.; Li, L. H.; Park, H. J.; Park, J. H.; Lee, K. Y.; Kim, M. K.; Shin, B. A.; Choi, S. Y. *Plos One* **2011**, *6*, e18556.
(4) MacNevin, C. J.; Gremyachinskiy, D.; Hsu, C. W.; Li, L.; Rougie, M.; Davis, T. T.; Hahn, K. M. *Bioconjugate Chem.* **2013**, *24*, 215.